Optimisation of Pre-set Forearm EMG Electrode Combinations using Principal Component Analysis

Kyle Gavin Hans McWilliam Fyvie

Johannesburg, October 2018

A dissertation submitted to the Faculty of Engineering and the Built Environment, University of the Witwatersrand, Johannesburg, in fulfilment of the requirements for the degree of Master of Science in Engineering.

The financial assistance of the National Research Foundation (NRF) towards this research is hereby acknowledged. Opinions expressed, and conclusions arrived at, are those of the author and are not necessarily to be attributed to the NRF.

Declaration

I declare that this dissertation is my own unaided work. It is being submitted to the degree of Master of Science in Engineering to the University of the Witwatersrand, Johannesburg. It has not been submitted before for any degree or examination to any other University.

....

(Signature of Candidate)

……………. day of ………………………… year ………………….

Abstract

Trans-radial amputees struggle daily when it comes to performing one or more of their activities of daily living (ADLs). Myoelectric prosthetic hands have recently been developed to a point where they can assist trans-radial amputees to perform their ADLs, making use of electromyographic (EMG) signals to drive the prosthetic hand. In order to function, a myoelectric prosthetic hand requires multiple electrodes to collect EMG data (denoted a channel) from a prosthetic user's remaining forearm muscles, as well as complex classification algorithms to process the data in real time. The focus of research in this field is directed at developing or improving the classification algorithms, often ignoring the optimisation of the EMG electrodes themselves. The electrodes can be optimised either by position or number, however in research where electrodes are optimised, classification accuracy is used as a measure of success for the optimisation, which requires optimisation of the classification algorithm itself.

The focus of the current study was to develop a method that could optimise the EMG electrode placements and number, without needing a classification algorithm. A pre-existing 8-EMG channel dataset for seven subjects was used. The experimental method involved generating combinations of two, three and four channels from which optimal channel combinations were selected. The optimisation process made use of principal component analysis (PCA), which generated a reduced-quality model for each potential combination. The reduced-quality and original models were compared, and the optimal channel combinations identified from those comparisons with the least error. The success of the optimisation was defined as the impact that a reduced number of EMG channels would have on the percentage of variance retained (PVR) by the optimal channel combinations.

The optimal channels for each subject were compared, and although each subject displayed variation, in general the important channels were identified as those that were located over the Extensor digitorum (ED), Flexor pollicis longus (FPL), Flexor digitorum superficialis (FDS), Flexor digitorum profundis (FDP), and

Extensor carpi ulnaris (ECU) muscles. The optimal channel combinations for all subjects together had an average of 64.5% PVR for the 2-channel setup, 73.9% for the 3-channel setup, and 76.5% for the 4-channel setup. This shows that it is possible to reduce the number of channels and retain a large amount of variance in the data without the use of classification algorithms.

Acknowledgements

I would like to start by thanking both of my supervisors, Prof Vered Aharonson and Mr Abdul-Khaaliq Mohamed. Their valuable advice most certainly shaped the course of this study, and upon the completion of this task I am very grateful for the guiding approach that they took to assisting me. Being guided to choose my own topic and define my own research goals and methods was tough to start with, but I am much more confident in my own abilities as a researcher because of them.

I would also like to acknowledge the National Research Foundation for the financial assistance that they provided over the course of this project.

I also want to thank my fellow researcher Gabriel for his company while going through this project, and I hope his journey is as successful as mine.

Lastly but not least, I want to express my appreciation for all the support I have received from my wife Carmen, my sister Robyn and my parents Guy and Nicky, throughout the process of completing this project. They have never doubted my ability to complete it, and have been waiting very patiently for the outcome. I’m truly glad to have a family like you.

Table of Contents

List of Figures

List of Tables

Glossary of Terms and Abbreviations

Abbreviation/Term	Full Name/Description
ADL	Activity of daily living
APL	Abductor pollicis longus
CC	Correlation coefficient
DOA	Degrees of actuation
DOF	Degrees of freedom
ECRB	Extensor carpi radialis brevis
ECRL	Extensor carpi radialis longus
ECU	Extensor carpi ulnaris
ED	Extensor digitorum
EMG	Electromyography
EPB	Extensor pollicis brevis
EPL	Extensor pollicis longus
FCR	Flexor carpi radialis
FCU	Flexor carpi ulnaris
FDP	Flexor digitorum profundis
FDP-L	Flexor digitorum profundis (lateral aspect)
FDP-M	Flexor digitorum profundis (medial aspect)
FDS	Flexor digitorum superficialis
FEM	Fixed effect model
FPL	Flexor pollicis longus
GA	Grasp analysis
HC	Hand close
I	Index finger
iEMG	Intramuscular electromyography
I-M	Index-middle
I-M-R	Index-middle-ring
L	Little finger
LDA	Linear discriminant analysis
M	Middle finger

MCA	Mutual component analysis
MI	Mutual information
M-R	Middle-ring
M-R-L	Middle-ring-little
MSC	Magnitude squared coherence
MUAP	Motor unit action potential
NAP	Nerve action potential
NRMSE	Normalised root mean squared error
PC	Principal component
PCA	Principal component analysis
PVR	Percentage variance retained
R	Ring finger
RA1	Research aim 1
RA1-P1	Research aim 1 – part 1
RA1-P2	Research aim 1 – part 2
RA2	Research aim 2
R-L	Ring-little
RMSE	Root mean squared error
RQ	Research question
sEMG	Surface electromyography
T	Thumb
T-I	Thumb-index
T-L	Thumb-little
T-M	Thumb-middle
TP	Time period
T-R	Thumb-ring

Chapter 1 – Introduction to Study

This chapter discusses the background to the problem identified for study in Section 1.1, followed by Section 1.2 which identifies the significance of solving such a problem. Lastly, Section 1.3 describes the structure that the remainder of this dissertation takes.

1.1 Background to Problem

Trans-radial amputation refers to the loss of any portion of the forearm through amputation [1]. This type of amputation can occur at several different levels of the forearm, meaning that different forearm amputees can have different degrees of residual limb remaining. These differences in degrees of amputation make it difficult to find a standardised way to assist trans-radial amputees. The challenge that trans-radial amputees face is the degree (if any) to which they can perform one or more of the activities of daily living (ADLs) [2]. ADLs involving the hand include writing (requiring fine motor control of the fingers), typing (requiring movement of the fingers), lifting a telephone receiver (requiring coarse motor control of the fingers) or pouring water from a jug (requiring stability of the hand) [2]. Each ADL requires the fingers to be manipulated in a specific way to achieve the desired performance. If an ADL requires the fingers/hand to be held stable for a period of time (such as holding a jug of water), as opposed to a transitional action (such as typing), the position the fingers maintain is known as a grasp. For some ADLs the grasps are very similar, for example lifting the telephone receiver and pouring water from a jug.

In order to simplify the analysis of ADLs, various sets of common grasps have been defined for the purpose of achieving the ADLs using a functional hand [3]–[5]. Some ADLs can be achieved using these common grasps [2], [3]. Other ADLs may require the use of a combination of the grasps together in order to generate a more complex or specialised grasp [4], [6], [7]. Often the grasps that are performed to achieve ADLs do not require the participation of all the fingers of the hand, such as the case of pressing a button with the index finger or pinching an object between the thumb and index finger.

Prosthetic hands can be used to assist trans-radial amputees in performing their ADLs. They are generally programmed to perform a set of grasps, using some form of input from a user. Of interest are myoelectric prosthetic hands that make use of electromyographic (EMG) signals as an information source for actuating the prosthetic hand into a grasp. EMG is the measure of electrical signals generated by muscle contractions, and are collected by electrodes that are placed on the surface of the users' skin, referred to as surface EMG (sEMG), to measure the underlying muscle [8], [9]. EMG electrodes can also be implanted in the muscles themselves, known as intramuscular EMG (iEMG) [10]. While iEMG may provide more accurate measurements of the electrical activity, the implantation requires invasive measures and this is often not desirable [10]–[12]. The physical EMG electrode is responsible for collecting data, and the collected data in digital form is known as an EMG channel.

Given recent progress in myoelectric prosthetic hand technology, multiple different prosthetic hands are commercially available [13]–[15]. The prosthetic hands are often complex, allowing for multiple degrees of freedom (DOF) and degrees of actuation (DOA) to be implemented [3], [16]. These allow for the programmed generation of many of the grasps needed for ADLs, including individual finger grasps, which until recently were beyond the prosthetic hands' capabilities [17]. This means that the prosthetic hands can be programmed to perform grasps with almost human-like dexterity, but enabling a user to control them with such accuracy in real-time presents a major challenge [16], [18].

The challenge with controlling a myoelectric prosthetic hand with a high accuracy in real-time is often the lack of informative EMG data that can be processed to generate the required control [19]. This can be due to a number of reasons, one of which is the limitation of potential EMG electrode placement sites on a trans-radial amputee's forearm [20], [21]. Studies often make use of more than five EMG electrodes to measure data [14], [16]. This provides a large amount of data that is often helpful with classification [22], [23]. However, it is not practical to make use of so many muscle placement sites for real-time EMG data acquisition. This is because there are often only two or three independent muscle placement sites available [24] on a trans-radial amputee.

There are generally two methods of overcoming this control challenge. One method considers the fact that the muscles normally responsible for some grasps may be atrophied or missing due to the amputation. Studies have made use of a mapping system that uses alternate forearm muscles usually reserved for controlling other grasps [13], [24]. These systems map the EMG channel measurements from these alternate muscles onto the grasps required to perform the ADLs. The problem with this type of system is two-fold: 1) The muscles in the mapping normally perform other grasps, so a user must learn to use these muscles for a different purpose. 2) The learning process is complex, so a user may have trouble using the prosthetic hand effectively and may reject it [3], [25].

The second method considers the use of a limited number of EMG channels as inputs to control the prosthetic hand. With such a method, the position of placement of EMG electrodes on a potential myoelectric prosthetic user's forearm becomes imperative to generate good-quality EMG channel data for classification. The success of such a system depends on what grasps are being classified, and which muscles are used to generate these grasps. The use of two EMG channels as an input is the minimum for any useful control, and a number of studies make use of this [3], [4], [13]. The successful use of a limited number of channels for EMG data collection requires that the selection of channels be optimised – in terms of both the physical placements of the electrodes on the relevant muscles, as well as the number of channels that are used for data collection.

Using intuitive-to-control myoelectric prosthetic hands can enable trans-radial amputees to perform grasps and achieve their ADLs. However, for the prosthetic hands to function properly, good-quality EMG channel data, collected from a limited number of electrode placement sites, is required. Identifying these optimal sites currently requires a lengthy and complex process of experimental placement and testing of the resultant EMG channel data. Additionally, the use of classification algorithms is generally required to validate the optimisation. A potential solution that identifies these optimal EMG electrode placement sites without the use of a classification algorithm needs to be pursued.

1.2 Significance

Many studies that make use of the collection of EMG channel data to control myoelectric prosthetic hands do not address the possible benefits of selecting an optimal combination of EMG channels. This may be largely due to the focus of these studies on the classification of the EMG data, rather than on the quality of the data. This is because being able to successfully classify sub-optimal data means that the classification system is robust. Some of the studies that do discuss optimal electrode placements [17], [26] use a classification system to measure the success of the optimisation. This poses the challenge of having to optimise the classification system in addition to the EMG channel selection to be sure that the results are accurate.

This study aims to identify a new method for optimising the EMG electrode placement process. This process is to be done prior to the use of a classification algorithm, to confirm that the EMG channel optimisation was successful. In addition to determining the most important EMG channels to use for a given set of grasps, the underlying relevant muscles can also be identified so that future classification systems may base their EMG electrode placements on the results of this study.

1.3 Dissertation Structure

This study aims to answer the following research question (RQ): In using an 8-channel EMG dataset, what are the optimal combinations of two, three and four EMG channels that preserve their data variance content when compared to the original 8-channel dataset?

To answer this question fully, the study is split into two main research aims (RAs). Research aim 1 (RA1) is as follows: What are the optimal two, three and four channel combinations for each subject within the dataset, and how good is it compared to the original 8-channel dataset for each subject? And research aim 2 (RA2): Given the two, three and four channel optimal combinations identified in RA1, which muscles are mainly responsible for generating this EMG data?

Figure 1.1 indicates how the RQ was broken down into goals. The splitting of RA1 into two parts (RA1-P1 and RA1-P2) is discussed when looking at the overview for Chapter 4 and Chapter 5. The process of answering the RQ is as follows: RA1-P1 is used to answer RA1-P2, and they together answer RA1. Then RA1 is used to answer RA2, and they together answer the RQ.

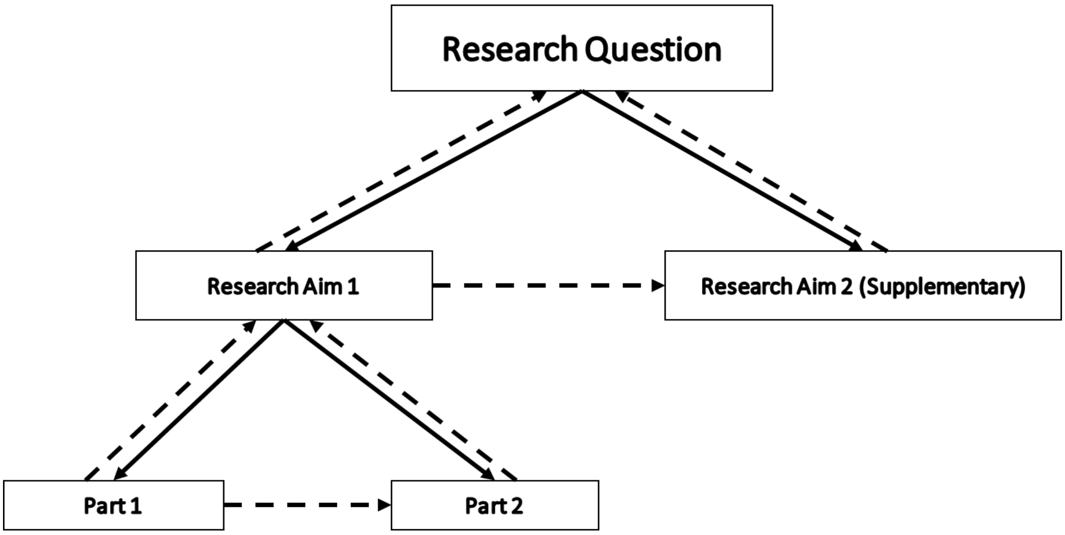

Figure 1.1: Flow diagram of research goals. Solid lines indicate a splitting up of goals into smaller parts, dotted lines indicate the use of smaller goals to answer their parent goals.

To answer these RAs and subsequently the RQ, the rest of the study is structured as follows:

Chapter 2 looks at the prominent techniques in this study, namely EMG and principal component analysis (PCA). It explains the concepts behind these technologies and reviews the relevant literature to define the RQ. In addition, the background of the signal error metrics used in this study and their definitions are reviewed, followed by a description of the relevant anatomical muscular structures of the forearm.

Chapter 3 describes the 8-channel EMG dataset that was used for this study, including the subjects that participated in the data collection experiment, and the hardware and software used. The chapter further presents information regarding the placement of electrodes, specifies the limitations of the experimental procedures and validates the data.

Chapter 4 and Chapter 5 focus on the methodologies used in answering RA1, by splitting it into two parts, RA1-P1 and RA1-P2. The methodology in Chapter 4 (based on PCA), focusses on RA1-P1: What are the optimal channel combination trends that can be identified within and across subjects? Following this, Chapter 5 uses the results of Chapter 4 to focus on RA1-P2: How much impact does the reduction in the number of electrodes have on the variance content of the data?

Chapter 6 presents the results of both RA1-P1 (in a tabular format) and RA1-P2 (in a graphical format) for each subject that were generated by the methods in Chapter 4 and Chapter 5. Additional results derived from the individual subject results are presented for discussion.

Chapter 7 discusses the derived results presented in Chapter 6. Following the discussion, the various goals of this study are answered, using the structure identified in Figure 1.1.

Chapter 8 concludes the study and identifies potential future work.

Chapter 2 – Literature Review and Background

This chapter covers the various concepts and technologies that are used within the scope of this study. Section 2.1 and Section 2.2 cover the major topics that are tied directly to the title of the dissertation, namely: EMG and PCA respectively. Section 2.3 relates the RQ defined in Chapter 1 to the literature review of these major topics. Section 2.4 covers the background of other important concepts that complement the major topics, such as the signal error metric calculations used in this study and the relevant anatomy of the forearm muscles.

2.1 Electromyography (EMG)

Criswell discusses in [12] that the most basic level of organisation with regards to muscles is the motor unit, which includes a bundle of muscle fibres and their associated motor neuron from the spinal cord. A nerve action potential (NAP) will run through the neuron towards the muscle fibre. Upon reaching the muscle the NAP causes a depolarisation within the muscle fibre, which spreads throughout the muscle fibre, causing a contraction. This is what is known as a muscle unit action potential (MUAP). Several MUAPs acting together is what would more generally be known as a muscle contraction, and this depolarisation is what is being measured when using EMG. To change the strength of a contraction, a muscle may recruit different numbers of muscle fibres to be involved. The change in the number of recruited muscle fibres causes the amplitude of the corresponding EMG recording to change, since the EMG is recording the combined spatial and temporal depolarisations of the recruited muscle fibres, rather than a stronger depolarisation from a single muscle fibre.

There are two different forms of EMG, sEMG and iEMG [11], [12]. iEMG electrodes are implanted into individual muscles to generate more focussed recordings [11]. This is noticeable with the amplitude of the electrical signal, given that measurements using iEMG generate recordings in the range of millivolts versus using sEMG, which measures microvolts [12]. Specifically, the current study makes use of sEMG (referred to as EMG unless specified otherwise). It is safe and non-invasive and thus much easier to generate recordings, as the electrodes only need to be placed on the surface of the skin above the muscle that is being measured [8], [12]. Although the measurements are not as focussed on individual muscles or as strong amplitude-wise as iEMG, sEMG is still able to generate meaningful information. This is because muscles generally work in groups to achieve goals, a concept known as muscle synergy [27]. Muscle synergy in action is seen in Table 2.1, where multiple muscles work together to produce a grasp, and these muscles are involved in multiple other grasps as well.

Criswell discusses further [12]: Muscle fibres can work in different ways. There are three clearly identifiable types of muscle contractions: isometric, concentric and eccentric. Of interest here is the isometric contraction type, where a constant muscle length is maintained during contraction. Such a contraction is generally used for stability and postural control, or during manual muscle testing. EMG recordings are generally of highest amplitude when the muscle(s) measured are contracting in an isometric fashion.

2.1.1 Forearm EMG

Given that the muscles of the forearm are responsible for the movements of the hand at the wrist as well as most of the individual and combined finger movements and grasps, EMG measurement on the forearm is well documented [12]. Many studies look at using these EMG measurements as inputs for prosthetic hand controllers [3], [13], [16], [20], [26], [28], [29]. Understanding the control mechanisms employed to control the hand is vital to knowing which muscles become important when certain grasps or movements are performed [30], [31].

There are two general methods of electrode placement when measuring EMG on the forearm. The first is the general placement method, where the electrodes are placed on areas of the forearm (determined by anatomical knowledge) or around the circumference of the forearm [9], [16], [17], [26], [32], [33]. This method relies on the fact that the placement of the electrodes allows for differential EMG measurements to be taken. This assists in the classification process, since any classification algorithm relies on the differences within features to be successful [34]–[36]. The second method is to place the electrodes above specific muscles to measure them when they contract for a grasp [12]–[14], [37]–[39]. This method relies on the understanding of what muscles will contract to perform a grasp. This allows for a stronger EMG signal to be measured and processed for classification.

2.1.2 Optimal Electrode Combinations

The optimisation of EMG electrode placements is a focal point in the realm of EMG measurements used for prosthetic hands, and they can be optimised in multiple ways. These optimisations can be the choice of a correct placement of a single electrode to collect the best quality EMG data, the optimal spatial placement of several electrodes together, or the reduction of the total number of electrodes. Reducing the number of electrodes used in measurement is of particular importance, since a reduction in the number of required inputs for a classification system reduces its complexity [40]. The importance of the electrode placements and/or electrode reduction is largely contextual to the application and type of data collected. Even so, it is useful to be able to compare different datasets and identify which EMG electrode placement sites remain important throughout different studies.

Celadon *et al.* [33] made use of a linear discriminant analysis (LDA) classification system as a method for selecting an optimal reduced number of EMG electrodes. EMG data was collected from nine subjects using a sleeve of 192 electrodes, arranged in eight rings of 24 electrodes around the circumference of the forearm. The subjects performed tasks involving isometric contractions of the individual fingers of the dominant hand (not including the thumb), with a visual feedback of the force produced in their contractions. The tasks included both flexion and extension contractions while attempting to maintain force to prescribed levels. There were different inputs tested with the LDA classifier which included a single ring of the sleeve, two rings of the sleeve, determining the barycentre of EMG activity (referring to the centre of EMG activity on the sleeve) for each finger during the tasks, and lastly using all the electrodes available. The results of this study determined that using all the electrodes gave a classification accuracy of more than 91% on average. The performance of the barycentre and two-row methods was similar, producing a classification accuracy of approximately 82% on average. Lastly the single-row method gave the worst performance, with a classification accuracy of 75% on average. It is important to note that while the single row of electrodes had the worst performance, the use of eight EMG electrodes managed to give a performance that only had a 16% worse classification accuracy than using all the EMG electrodes. An explanation for this could be attributed to the lack of optimisation in the classification system for each subject, not necessarily the number of electrodes themselves. Even so, the Celadon *et al.* [33] study showed that a significant reduction in the number of electrodes was still able to extract most of the information that was present in the full electrode set.

Andrews [41] focussed on finger movement classification. This included optimising classifiers for each of twelve subjects, where data for this optimisation was collected from several typing tasks. It is noted that the generally-optimised classifiers performed worse than the classifier optimisation for each subject individually. This work extended into Andrews *et al.* [17] which focussed on selecting optimal EMG electrodes from a set of eight around the circumference of the forearm, using the optimised classifier for each subject. All possible combinations of eight electrodes were analysed for the classification accuracy. The results of this study determined that the electrodes placed on Flexor digitorum profundis (FDP) and Extensor digitorum communis (also known as Extensor digitorum (ED)) muscles were selected for most often overall. Some of the subjects didn't generate a classification accuracy above 50% until they used between five and seven electrodes. Even so, the Andrews *et al.* [17] study indicates that using seven electrodes gives a classification accuracy of 92.7%, which was not significantly different from the results achieved when using only three electrodes.

Khushaba and Kodagoda [26] proposed optimising the classification of fifteen finger grasps. Data was collected from eight subjects, using EMG electrodes placed around the circumference of the forearm. A combined feature selection and projection algorithm was proposed, called mutual component analysis (MCA).

MCA has two stages – firstly a mutual information (MI) algorithm is applied to determine the information redundancy between two features. If the MI between two features is high, then one of the features can be discarded without significant loss to data content. Once MI has been used to rank the features, a second stage using PCA is applied to remove noisy and redundant features, preserving the features that exhibit the most variance. The features preserved were run through several different classifiers to check classification accuracies. MCA reduced the original 168 features to between 42 and 44 features for the eight subjects. The classification accuracy for this study using the proposed method was above 95% on average across all subjects, using four or more EMG electrodes. This proves the success of the system with a greatly reduced number of EMG electrodes. The observation of the retained features identified that a particular subset of the eight electrodes used for data collection are important, namely those corresponding to ED, Extensor carpi ulnaris (ECU), and Flexor carpi ulnaris (FCU). The Khushaba and Kodagoda [26] study was limited to eight subjects, and so would need to be expanded in future work to validate the results.

Hargrove *et al.* [19] investigated the use of iEMG vs sEMG in a classification system. Six subjects were used, performing ten different movements of the hand and wrist. Each subject had sixteen sEMG electrodes spaced equally around the circumference of the forearm (the experimental setup used unipolar electrodes, so there were fifteen EMG channels), as well as six iEMG electrodes implanted in muscles. This facilitated the simultaneous collection of EMG data from both sources. Using multiple classification methods, the study determined that there was no difference between using six iEMG electrodes and using sixteen sEMG electrodes. The second part of this study involved identifying optimal sEMG electrode placements. The study used two different approaches, the first being a symmetrical selection of subsets of the original fifteen channels, and the second being a brute-force selection of all possible subsets. Using the symmetrical method identified that there was no benefit to having more than four electrodes; using the brute-force method determined that there was no benefit to having more than three electrodes. The optimal electrode subsets were investigated and the most important muscles for EMG collection were identified as the Supinator, FCU and Flexor digitorum sublimis, also known as Flexor digitorum superficialis (FDS). Using only three channels, the study could achieve an average classification accuracy of 97%. It is noted that the iEMG signals measured were measured from surface muscles, except for ECU.

2.2 Principal Component Analysis (PCA)

PCA is the process of analysing a data table in order to extract important information that is often not clearly seen in the data [42]. This data table is a matrix **X** with rows *I* and columns *J*, where each row corresponds to an observation, and each column corresponds to a variable [42]. PCA decorrelates this multivariate data and projects it onto a new orthogonal coordinate system, by using the variance exhibited by the variables [43]. The new coordinate system is defined according to diminishing variance, where the first dimension is the direction in which the original data exhibited the highest variance, and the orthogonal dimensions will exhibit diminishing variance of the original data [43]. Viewing the data on this new coordinate system allows for correlations/redundancies in the data to be more clearly seen, and compression of the data can be performed without losing too much of the information within the original data [44]. Compression in this context refers to the removal of dimensions/axes that explain to a lesser degree the variance in the data as a whole, leaving only a subset of the dimensions from the original system [42]. To achieve this, it is common practice to keep only a few of the highest variance dimensions that together explain a desired amount of variance. The rest of the dimensions are removed from the data [45].

Smith [44] briefly describes the process of performing PCA. Once some form of multivariate data has been collected, the mean of each column *J* is subtracted from the values for that column. This ensures that the dataset's mean is zero, which is important when considering that some variables may exhibit a form of bias. The covariance shown in Equation 1 (adapted from [44]) is calculated between each column in *J*:

$$COV(x, y) = \frac{\sum_{i=1}^{n}(x_i - \bar{x})(y_i - \bar{y})}{(n-1)} \tag{1}$$

Where x and y are the columns being compared, and n is the number of observations (number of rows I). The calculation of the covariance between all columns J generates a covariance matrix.

Each column of the covariance matrix represents an eigenvector, and each eigenvector has an associated eigenvalue. The eigenvectors are re-ordered from high to low according to their eigenvalues. The eigenvalues represent the amount of variance that is described by the new coordinate system, the axes of which overlap on each of the eigenvectors. These re-organised eigenvectors and eigenvalues are denoted the principal components (PCs). The data can then be mapped onto this new coordinate system, which will more clearly show the variance in the data, shown in a 2-dimensional example in Figure 2.1. In addition, dimensions that display minimal amounts of variance can be removed, so that the data can be viewed with only the most important variances present.

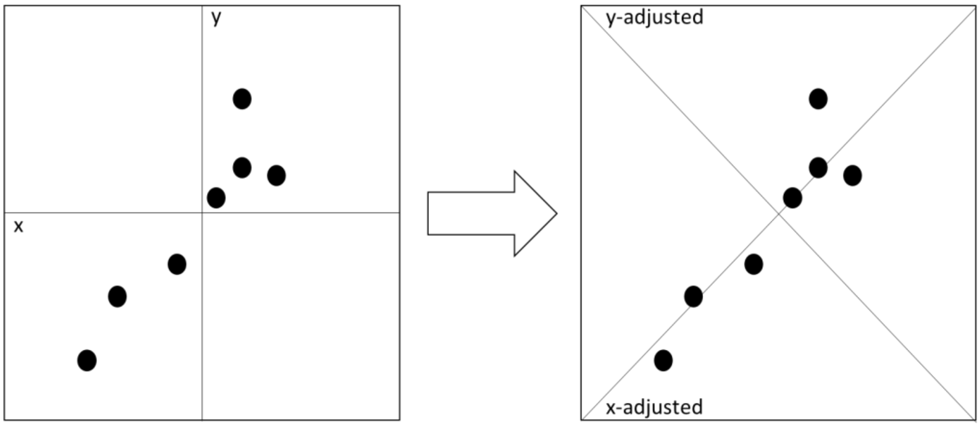

Figure 2.1: Adjusting on axes based on direction of greatest variance (the values are zero-meaned).

Smith [44] further describes how the removal of minimal-variance dimensions can be viewed in light of their impact on the data in the original coordinate system. This is particularly important when the PCA transform is used for data compression. The covariance matrix that was previously generated is used to reverse the mapping of the data, and the original mean is added back in to give the data points their original bias. Now that the reduced-dimension data has been remapped to the original coordinates, it can be visualised and compared to the original-dimension data.

It is important to note the terminology that EMG studies generally use for PCA. The variables of the columns J correspond to the specific EMG channels. Each observation in the row I corresponds to a timestamp within the collected EMG data.

2.2.1 PCA on EMG Signals

PCA is often used as an analysis tool for EMG signals, more specifically in the current study, the forearm muscles. The large number of muscles in the forearm don't work independently, rather they assist each other to achieve tasks [46]. This is known as muscular or neuromotor synergy, which is a common basis for the use of PCA on EMG signals, since PCA is able to identify these synergies [6]. Muscular synergy may be broadly defined in two categories [47]. Goal-directed synergy considers a unit (of synergy) to consist of components (in this case, muscles) that work together to form a net output [47]. The muscles of the synergy unit may work in different spatial and temporal combinations, but any synergies developed are considered to be equivalent so long as the net outputs are the same [47]. The other synergy is morphological synergy, which focuses on the importance of the spatial and temporal activity of the individual muscles [47]. In contrast to goal-directed synergy, two synergies are not considered to be equivalent unless their spatial and temporal profiles match exactly [47]. Musculoskeletal systems in general have many DOFs. The implementation of a controller that can map a nearly infinite number of behavioural movement goals onto an equally large number of muscle contractions can be extremely difficult [27]. Muscle synergy and PCA are techniques used to reduce the number of dimensions that such a system needs to process. In particular, goal-directed synergy is used since it can describe the same set of muscles differently depending on their activation sequences [27].

Artemiadis and Kyriakopoulos [48] focussed on a three-dimensional mapping of the shoulder and elbow joints using a magnetic position-tracking system. This mapping is correlated to the activation of nine muscles, which are all measured using EMG. The use of PCA in this study is two-fold: 1) To reduce the dimensionality of the EMG data, since the first and second PCs contained 95% of the variance data, and 2) to reduce the dimensionality of the joint angle data, where the first and second PCs contained 93% of the variance data.

Zhang *et al.* [49] based their study on the dimensionality reduction achieved by Artemiadis and Kyriakopoulos. The study reported that it was only possible to reduce from eight dimensions of EMG to five, while maintaining 95% of the variance data. This dimensionality reduction is applied before the generation of features for a classification system. PCA is noted for having an impact on the classification accuracy of the motions investigated, however the movements investigated were of the shoulder and elbow joints. The discussion of the Zhang *et al.* study evaluates this use of PCA on EMG signals for dimensionality reduction.

2.2.2 Fixed Effect Model in PCA

A fixed effect model (FEM) is a popular statistical model, that assumes that there is only one true effect that interacts with all the observations or timestamps in an analysis. All the observed differences in this effect are due to a sampling error (also known as noise as discussed in Section 2.4.1) [50]. In the context of an FEM, PCA is descriptive, where the amount of variance within the timestamps are explained by the PCs, and the amount of variance described by a PC indicates its importance [42]. Using PCA as an FEM means that the quality of the PCA model can be assessed by comparing a reduced-dimension model (as described in Section 2.2.1) to the original data [42]. Studies often derive new metrics that can be used to assess the models, and determine the optimal number of dimensions that the system can be reduced to [42], [45], [51].

All previously discussed studies that made use of PCA as an FEM aimed to identify how many PCs are required to retain a certain amount of variance. Those PCs that were not required to meet this goal are removed from the model. This is known as dimensionality reduction. They have not placed a restriction on the number of PCs that need to be retained. The current study does not use PCA to reduce dimensionality (with a variable number of PCs), but instead places a restriction on the number of PCs intentionally to reduce the quality of the reduced-dimension model. This allows for a greater deviation in values when compared to the original data. When the data is reconstructed to the original coordinate system, the deviation in data quality allows the original-dimension model and the reduced-dimension model to be compared using some form of error metric. A minimal error in this case indicates that the reduced-dimension model more accurately resembles the original-dimension model. Multiple error metrics are used in the current study for this purpose, which are described in Section 2.4.1.

2.2.3 Data Variance Content of Selected PCs

As discussed, PCA operates on the variance that the analysed data exhibits. Covariance is a measure of the variance that is exhibited by two variables [44]. To extend the concept of covariance further, a covariance matrix is used where all variables are represented on the row and column, and the cells are filled with the computed covariances of all variable pairs [44].

The trace of a square matrix refers to the sum of all the diagonal elements in the matrix [52]. In a covariance matrix these diagonal elements are the variances of each individual variable, thus the trace is a measure of the total amount of variance exhibited by all the variables of the covariance matrix [52]. To determine how much variance is attributed to a subset of variables, the variances of the variables in question can be divided by the trace of the covariance matrix and presented as a percentage [53]. This process is useful to determine the relative contribution of each variable to the information content of a system in terms of variance [53].

2.3 Literature Review Summary

The studies involving EMG generally attempted to use the acquired EMG data as inputs to classification algorithms. The classification algorithms were used to drive a myoelectric prosthetic hand. In each of these studies, there is an optimisation of the EMG electrode placement and/or the number of EMG electrodes, making use of the classification accuracy as a metric for success. The current study attempts to achieve an optimisation without resorting to the use of a classification algorithm to verify the success of the optimisation.

Each of the studies discussed in this chapter introduced some form of optimisation for their EMG data, and their results suggested that most EMG datasets can be optimised. In particular, the data used in the current study is provided by Khushaba and Kodagoda [26]. Where they used a classification system to optimise the number of EMG electrodes, the current study did not use a classification system. Additionally, the muscles that contributed most to the optimised EMG data were identified by Khushaba and Kodagoda [26]. This allowed for a comparison between an established classification-based method and a potential non-classification based method.

PCA is frequently used in EMG processing applications, but usually in the form of determining a limit for dimensionality reduction for a classification system. In the current study, PCA was used as an FEM, and the original-dimension and reduced-dimension models were compared on a variable-by-variable basis using the three signal error metrics described in Section2.4.1.

2.4 Background

The following subsections relate to other concepts and techniques that were used in the current study, namely signal error analysis and muscles of the forearm.

2.4.1 Signal Error Analysis

Three signal error metrics were prominently used to compare original EMG signals to 2-PC reconstructed signals, namely: normalised root mean squared error (NRMSE), correlation coefficient (CC) and magnitude squared coherence (MSC). The reconstructed EMG signal is considered to have only one type of error – noise [54]. This is due to the fact that the two signals being compared are not compared from a cross-session perspective, which reduces the presence of bias and scaling errors [54]. NRMSE and CC metrics are chosen for their ability to measure noise effectively, and are measured in the time domain [54]. MSC is a measure of the energy distribution in the frequency domain [55].

The use of multiple error metrics in combination allows for a “majority vote” to be applied when choosing optimal channel combinations. This voting system also helps resolve cases where the three error metrics do not always converge to the same optimal channel solution. Each error metric is given the same weighting for this study. Considering alternative weightings for the error metrics is beyond the scope of this study, and is discussed in Section 7.7.

Normalised Root Mean Squared Error

This metric is a variation of the more general root mean squared error (RMSE). Normalising the RMSE avoids potential problems that can arise if the datasets that are being compared have differing scales [54], [56]. The equation for the NRMSE can vary depending on what measure the RMSE is divided by for the normalisation [54], [56]. The NRMSE used in the current study is shown in Equation 2 (adapted from [57]):

$$NRMSE = \sqrt{\frac{\sum_{n=1}^{N}[o(n) - r(n)]^2}{\sum_{n=1}^{N}[o(n)]^2}} \qquad (\mathbf{2})$$

Where *o(n)* is the original EMG signal, *r(n)* is the reconstructed EMG signal, and *N* is the number of time points over which the analysis was performed. The error value is generally found to be between 0 and 1, but in cases where *r(n)* and *o(n)* are completely opposite the error value may be greater than 1.

Correlation Coefficient

This metric measures how closely two signals change with each other. In this case, the output from Equation 3 (adapted from [57]) needs to be as big as possible, indicating a close relationship.

$$CC = \frac{cov(o,r)}{\sigma_o \sigma_r} \qquad (3)$$

Where *cov(o,r)* is the covariance of the original EMG signal and the reconstructed EMG signal. σ_o and σ_r are the standard deviations of the original EMG and reconstructed EMG signals respectively. The output value is bound between 0 and 1.

Magnitude Squared Coherence

This is a measure of the correlation between two signals based on their energy distribution in the frequency domain [55]. In this case, the output from Equation 4 (adapted from [57]) needs to be as big as possible, indicating a close relationship in terms of the frequency content.

$$MSC = \frac{|P_{or}(f)|^2}{P_o(f)P_r(f)} \quad (4)$$

Where $P_{or}(f)$ is the cross power spectral density of the original EMG signal and the reconstructed EMG signal. $P_o(f)$ and $P_r(f)$ are the power spectral density of the original EMG signal and the reconstructed EMG signal respectively. The output value is bound between 0 and 1.

2.4.2 Muscles of the Forearm and Grasping

The discussion in this section is based on Moore *et al.* [46]. To understand the hand movements and grasps used to perform ADLs, an understanding of the musculature involved is needed. Muscles are only able to pull in a single direction during contraction, so the degree of involvement that a single muscle has in performing a grasp is strongly correlated to its location. The largest group of muscles involved in performing movements related to the fingers are in the forearm.

Commonly, the forearm is divided into two compartments, namely the flexor compartment and the extensor compartment. These compartments are split by the ulna and radius bones, along with the interosseous membrane between the two bones. The flexor compartment contains the muscles involved in flexing the fingers or closing the hand. The extensor compartment houses the muscles involved in extending the fingers or opening the hand. Table 2.1 lists the main muscles of the forearm involved in these movements, excluding some of the more specialised, smaller muscles that are not considered relevant. Note that this study is only concerned with the flexion and extension of the finger; however, the listed muscles also perform other actions such as flexion and extension of the wrist. These movements are not relevant to this study and are therefore excluded.

Table 2.1: Forearm muscles and their actions.

Compartment	Muscle Name	Shorthand Name	Action(s)
Flexor	Flexor digitorum superficialis	FDS	index, middle, ring and little finger flexion
	Flexor digitorum profundis (lateral)	FDP-L	index and middle finger flexion
	Flexor digitorum profundis (medial)	FDP-M	ring and little finger flexion
	Flexor pollicis longus	FPL	thumb flexion
Extensor	Extensor digitorum	ED	index, middle, ring and little finger extension (all together is hand opening)
	Extensor carpi radialis longus	ECRL	hand closing
	Extensor carpi radialis brevis	ECRB	hand closing
	Extensor carpi ulnaris	ECU	hand closing
	Abductor pollicis longus	APL	thumb extension
	Extensor pollicis brevis	EPB	thumb extension
	Extensor pollicis longus	EPL	thumb extension

The flexor compartment is split into three layers; the surface layer, the intermediate layer, and the deep layer. The surface layer contains no muscles involved in the hand and finger movements. Figure 2.2 shows the right forearm anteriorly, from the surface perspective.

Figure 2.3 shows the third, deep layer of the right forearm with surface muscles removed.

The extensor compartment also has layers, but the muscles involved in the finger and hand movements are on the surface, and so can be seen in Figure 2.4, which shows the right forearm posteriorly. Note that what is displayed as ED in fact includes a smaller muscle, Extensor digiti minimi, but for the purposes of this study this muscle performs it actions alongside ED.

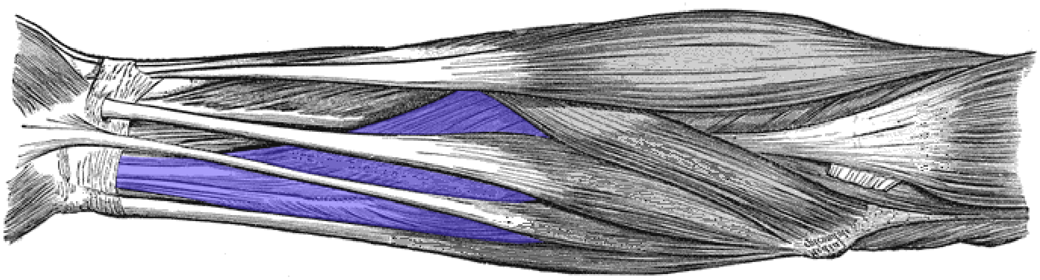

Figure 2.2: FDS muscle (blue) below the anterior surface layer (Adapted from [58]).

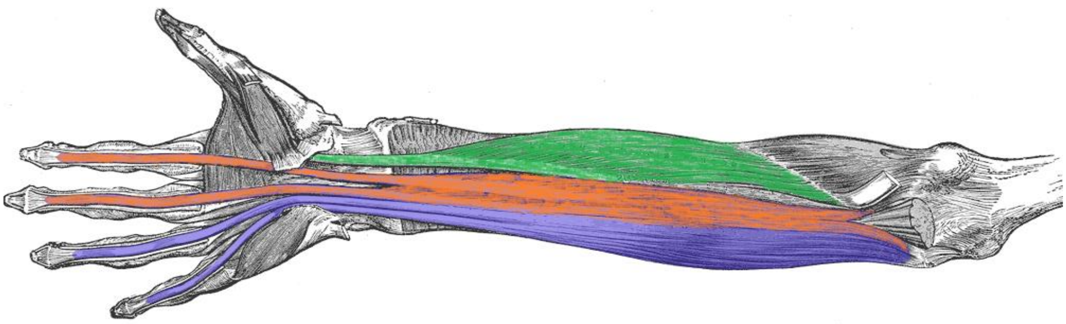

Figure 2.3: FDP-M muscle (blue), FDP-L muscle (orange) and FPL muscle (green) of the anterior deep layer. Note the distinction between the medial and lateral parts of FDP, because the index and middle fingers are flexed by FDP-L and the ring and little fingers are flexed by FDP-M (Adapted from [59]).

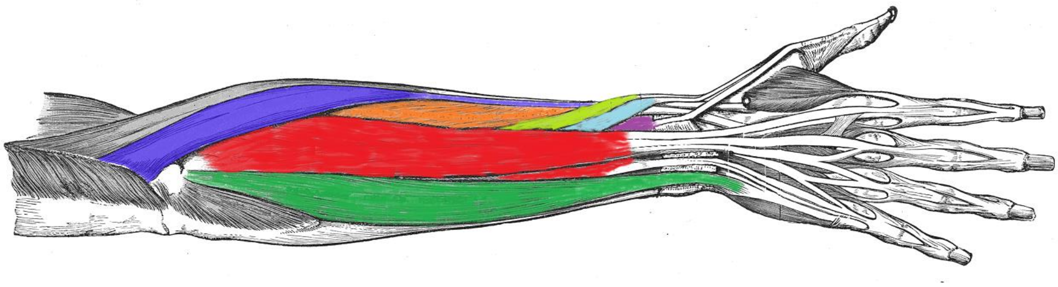

Figure 2.4: ECRL (blue), ED (red), ECU (green), ECRB (orange), EPL (purple), APL (light green) and EPB (light blue) of the posterior surface layer (Adapted from [60]).

2.5 Chapter Summary

EMG is conceptually important to the current study, as it was the method with which the experimental data was collected, as detailed in Chapter 3. The studies involving EMG data were focussed on the optimisation of EMG electrodes, through selecting a reduced number of electrodes and/or identifying important EMG electrode placement locations. All these studies made use of some form of classification algorithm to produce a result as to how effective the optimisation was. The current study attempts to avoid the use of a classification algorithm. It relies rather on PCA as an FEM to identify important PCs and their variances to identify optimal electrode locations and channel combinations.

Lastly, the anatomical structure of the relevant forearm muscles is discussed in general. This is vital to understanding which muscles are involved in which different types of grasps, when using individual or combinations of fingers. The correspondence of these muscles to the EMG electrodes used in the dataset is discussed in Chapter 7, where the optimal channel combinations are discussed. By extension of having the optimal channel combination results, the active muscles were identified.

Chapter 3 – Experimental Setup

This chapter describes and discusses the dataset that was used in the current study. No EMG data collection was performed. Rather a suitable EMG dataset was identified and used. Section 3.1 discusses the source that supplied the data. It includes the details about the subjects, the hardware and software used, the relevant muscles and EMG electrode placements and lastly the experimental procedure that was used to collect the EMG data. Section 3.2 discusses the limitations of the dataset, as well as validations performed.

3.1 Dataset

The data used in this study was made available by Khushaba and Kodagoda [26]. Permission for use of this data was provided in the EMG Datasets repository [32], provided that the corresponding paper is cited. Ethics clearance for the use of the EMG data was provided by the University of the Witwatersrand, provided in Appendix A with ethics clearance certificate number M161180. All details discussed in Sections 3.1.1, 3.1.2 and 3.1.4 are provided by Khushaba and Kodagoda [26] and the EMG Datasets repository [32].

3.1.1 Subjects

A total of eight subjects (six males and two females) participated in the data collection process of Khushaba and Kodagoda [26]. The subjects' ages ranged from twenty to 35, had no limb abnormalities or amputations, and had no neurological or muscular disorders. All the participants of the study provided informed consent prior to their participation in the study.

3.1.2 Experimental Setup, Hardware and Software

Subjects were seated on an armchair, with the arm supported and fixed at one position for the duration of the data collection process. EMG data was recorded using eight EMG bipolar electrodes (DE 2.x series EMG sensors) that were mounted around the circumference of each subject's forearm, using a two-slot adhesive skin interface to stick the sensors firmly to each subject's skin. A conductive adhesive dermatode reference electrode was placed on the wrist of each subject, on the same arm that the EMG data was recorded from. The collected data was amplified to a total gain of 1000 (Delsys Bagnoli-8 amplifier). A twelve-bit ADC (National Instruments, BNC-2090) sampled the signal at 4000 Hz, and the data was acquired using the Delsys EMGWorks Acquisition software. The data was processed by the Bagnoli desktop EMG system (Delsys Inc), with a bandpass filter between 20 Hz and 450 Hz and notch filter at 50 Hz to remove line noise.

3.1.3 Electrode Placements on the Forearm

Note that the electrodes used to collect the data were surface EMG electrodes. The muscles involved in the hand and finger grasps are not always located near the forearm surface, and are often located below other muscles. To associate an EMG electrode with a muscle found deep in the forearm, the muscle located on the surface of the forearm between them is considered. It is reasonable to assume that the signal associated with a finger or hand movement can generally be picked up by the EMG electrode(s) closest to it. Thus, when an electrode measures an EMG signal, the use of anatomical knowledge on muscle positions and inter-relations can generally identify the deeper muscle responsible.

The dataset originates from Khushaba and Kodagoda [26], [32], and provides no reference to the surface muscles the EMG electrodes were placed on. However, a study by Naik *et al.* [61] – which also makes use of this EMG dataset – have proposed the following surface muscle to EMG electrode associations in Table 3.1.

Table 3.1: Naik *et al*. [61] surface muscles and their corresponding EMG electrodes for the dataset provided by Khushaba and Kodagoda [26].

Electrode(s)	Surface Muscle
1	ED
2 and 3	Brachioradialis
4	Flexor carpi radialis (FCR)
5, 6 and 7	FCU
8	ECU

Additionally, Naik *et al.* [61] proposed that electrodes 1, 2, 7 and 8 be considered as being located on the posterior aspect of the forearm, where electrodes 3, 4, 5 and 6 are placed on the anterior aspect. In most respects the associations in Table 3.1 as well as the anterior/posterior identification are carried into the current study, however some changes to these associations have been proposed and implemented. These differences are covered in Chapter 7.

3.1.4 Experimental Procedure and Results

A total of fifteen different finger movements were investigated, as shown in Figure 3.1. The movements include flexion of the individual fingers: thumb (T), index (I), middle (M), ring (R) and little (L). Additional movements are combinations of fingers: thumb-index (T-I), thumb-middle (T-M), thumb-ring (T-R), thumb-little (T-L), index-middle (I-M), middle-ring (M-R), ring-little (R-L), index-middle-ring (I-M-R), middle-ring-little (M-R-L) and a full hand close (HC).

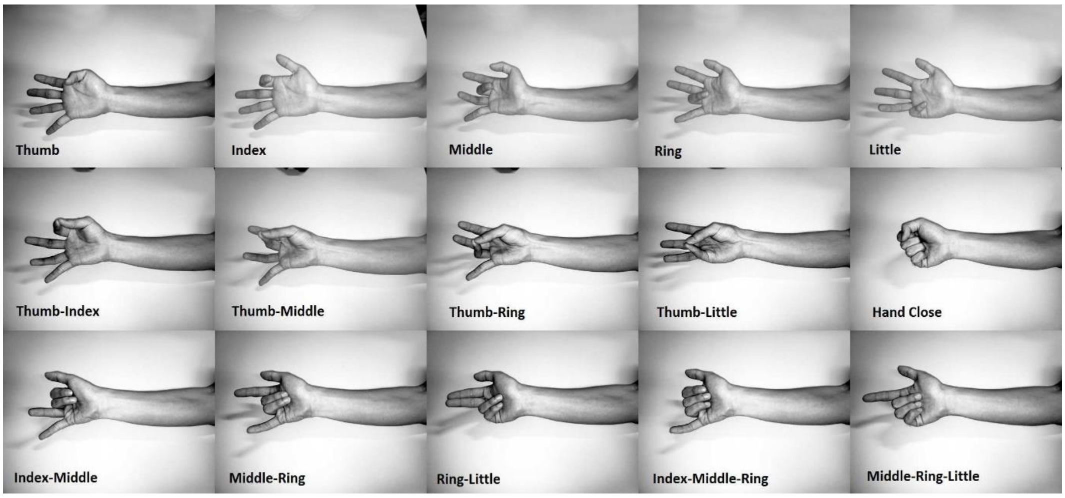

Figure 3.1: Individual and combined finger grasps investigated by Khushaba and Kodagoda [26] (with permission).

During the data collection process, each subject performed a total of six trials per grasp (although only three were made available for public use). A single trial consisted of holding a grasp for a period of twenty seconds (only the first five seconds were used in Khushaba and Kodagoda [26]). The EMG signals were made available in the form of csv files, where each file was a single trial for a single grasp for a single subject. The files consisted of the raw data points that were taken over the twenty second period.

3.2 Data and Function Validation

Matlab 2015b was used to import the data from the csv files and to perform all the processing that will be discussed in this section, as well as in Chapter 4 and Chapter 5. Some processing was performed on the data before it was made available for public use as described in Section 3.1.2. The quality of the resulting data needed to be assessed and therefore the following validation process was initially performed:

Visual Inspection of Channel Data

The data was visualised to ensure that each csv data file contains valid data for each grasp for each subject. Figure 3.2 shows a typical time-series plot that was used for this visual validation. During the visualisation, it was noted that the datasets for Subject 6 and Subject 7 were the same for some of the grasps, and in other cases Subject 6's data did not look similar in structure to any of the other subjects. For this reason, it was decided to omit Subject 6's data from the study.

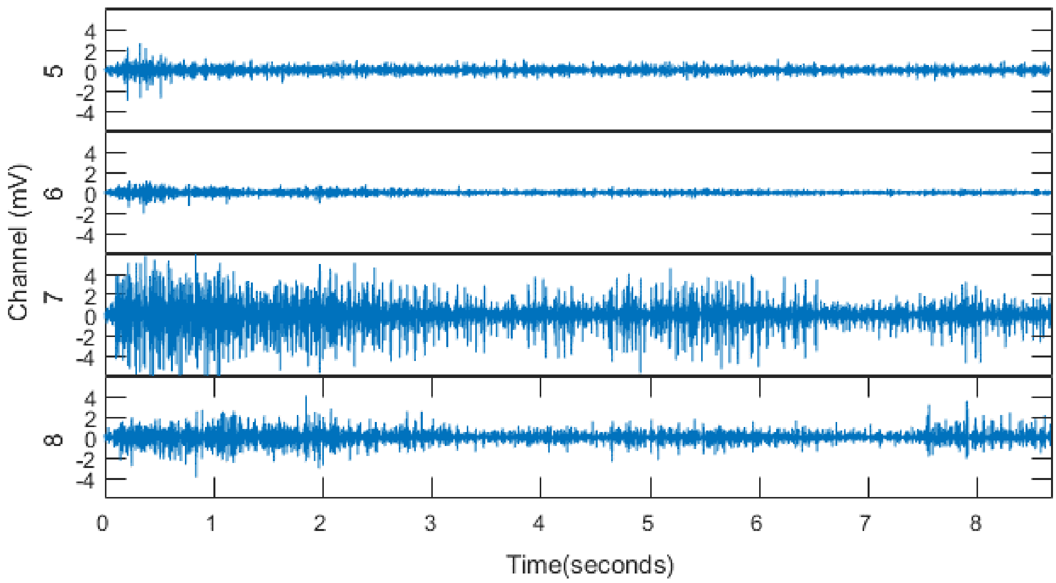

Figure 3.2: Typical time-series plot of EMG data for some channels within a short time period.

Data Length

Given that twenty seconds of data was collected per grasp at a sampling frequency of 4000 Hz, each grasp should have 80 000 data points per channel. This was confirmed using a counting script.

Data Filtering

The spectra of the data were inspected using a Matlab FFT script to validate the 20 Hz to 450 Hz bandpass filter as well as the 50 Hz notch filter. It appeared that the 20 Hz and 450 Hz filters had been implemented, but in some cases a 50 Hz peak was apparent in the data, implying that the notch filter was either missing or inefficient in the data provided. To correct this, a 50 Hz notch filter was applied to the data. A typical example of the frequency structure of the data can be seen in Figure 3.3.

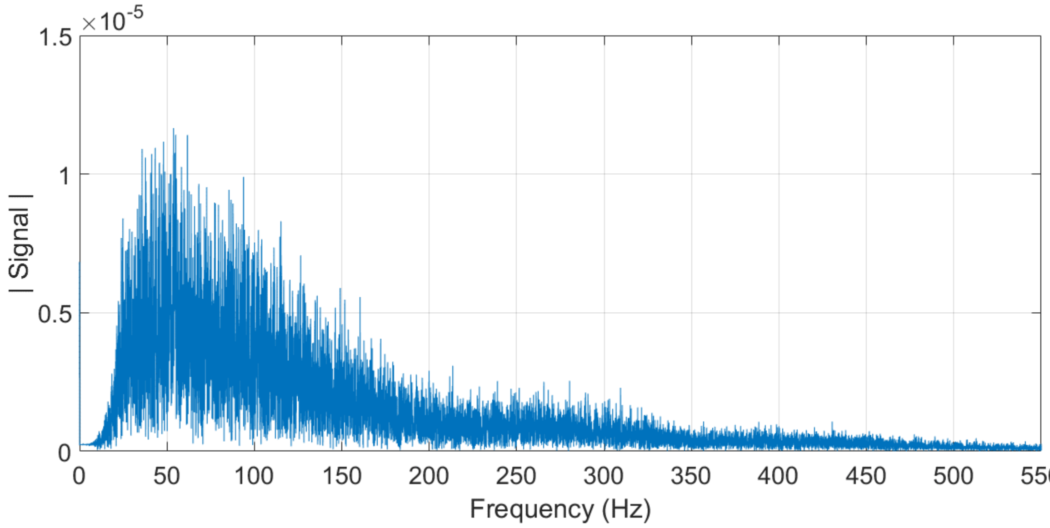

Figure 3.3: Typical FFT plot of a channel (Subject 8, Trial 3, M Grasp, Channel 5).

Limitations of the Dataset

Although this dataset was suitable for the purposes of the current study, several limitations were found. There was a limited number of subjects that participated in the data collection process. This restricted the conclusions reached in this study. The demographics information on the participants was not disclosed, although with such a limited number of participants this may not have been useful in any case.

In terms of the experimental setup, the order and type of filters used for processing the EMG data were not disclosed. This means that the experiment itself could be difficult to replicate if desired.

The experimental procedure did not mention any rest period(s) provided to the subjects between the recording sessions, so fatigue might have had an unknown impact on the EMG recordings. Additionally, there was no indication whether the grasp being recorded was initiated before recording began, or as the recording started. Lastly, there were no recordings during a rest period, which could have been used as a baseline for comparative purposes.

Matlab PCARES Function Validation

The PCA algorithm is a central component of this study. To ensure that the use of the PCARES function in Matlab would provide acceptable results, a manually-written function was built from PCA's first principles. This function and the PCARES function were both applied to the same dataset to validate that Matlab's function performed exactly as the PCA algorithm was understood to perform.

3.3 Chapter Summary

This chapter described the dataset that was selected for use in the current study. The information was based upon the source that provided the dataset: Khushaba and Kodagoda [26]. It included details of the equipment used, the subjects and the experimental setup. The information was lacking in some respects, and notes were taken for consideration in the current study. Validation methods were applied to ensure that the data was in a good-quality state, and in cases where the data was found to be corrupted or inadequate (as in the case of Subject 6), the data was excluded from the current study. In addition to the validations on the data, Matlab's built-in PCARES function was validated.

Chapter 4 – Methods for Identifying Optimal Channel Combinations

Chapter 4 and Chapter 5 discuss the methodology that produced the results presented in Chapter 6. The methods of Chapter 4 focus on RA1-P1: What are the optimal channel combination trends that can be identified within and across subjects? Chapter 5 deals with the RA1-P2.

The method employed here aimed to identify optimal channel combinations for each subject, if only two, three or four EMG electrodes out of the original eight EMG electrodes were available. The original grasps of the EMG dataset were mapped into groups, denoted Grasp Analyses (GAs). The results consider each GA and its associated optimal channel combination for the cases of a 2-channel, 3-channel or 4-channel setup. They are displayed in tabular format. In all the results, the channel combinations are a subset of the original eight channels that were used by Khushaba and Kodagoda [26], [32] to collected the EMG data.

The method overview is portrayed in Figure 4.1. Each section in this chapter details a block element. Input Data refers to the pre-processed data discussed in Chapter 3 and so will not be repeated in this chapter.

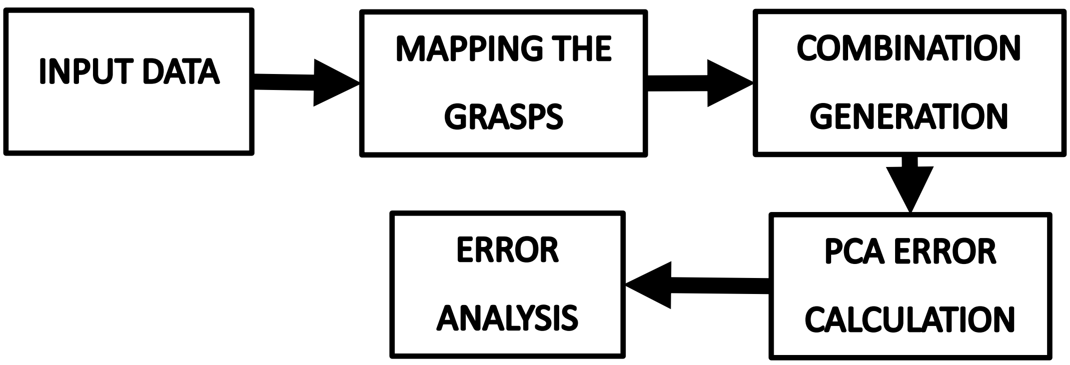

Figure 4.1: Method overview - the five block elements are each discussed as a section in Chapter 4 (except for the Input Data block).

4.1 Mapping the Grasps

A total of fifteen different grasps for each subject were investigated by the dataset providers Khushaba and Kodagoda [26], [32] as discussed previously in Chapter 3. Each of these grasps includes data for the eight channels that were placed around the forearm of the subject during the data collection process. Each subject has three trials for each grasp. To reduce the number of signals to analyse and reduce noise in the signals, the current study averaged the three trials on a channel-by-channel basis. To provide an analysis that was focussed on the EMG contributions for each finger of the hand, the fifteen grasps were firstly grouped into three categories. The three categories of GA are *All Grasps*, *Single Grasp* and *Focal Grasp*. Each category has a specific pattern in terms of which grasps were used in a GA. *All Grasps* considered all the grasps together, *Single Grasp* considered only the individual finger grasps, and *Focal Grasp* included all the grasps related to the "focal finger". Table 4.1 summarizes this mapping.

The *All Grasps* category contains a single GA – All Grasps - which encompasses all the grasps together. This GA would typically be done to identify the optimal channel combination in a straightforward manner when it comes to training a classification system. Since the *All Grasps* category obviously includes grasps that are present in the other GAs, often the *All Grasps* GA yielded similar optimal channel combinations to some of the other GAs, though this was not always the case. The *All Grasps* GA was overall considered to be the best determinant for identifying the optimal channel combinations, since it includes all the grasps. The other GAs served to confirm this as well as provide insight into the more specific channels that become more relevant with specific GAs.

The *Single Grasp* category of GAs contains only grasps that relate specifically to the use of a single finger. Given that there are five grasps in the original fifteen that meet this criterion, there are five GAs that map exactly from the grasps to the GAs. These GAs were used to identify which channels are important for each individual finger, and these important channels were expected to be different for the different fingers. There were cases where different GAs identify the same channels as being important, most notably in the case of any combination of the middle, ring and little fingers, since these fingers tend to use muscles that are closely anatomically related. These muscles are the FDS and FDP, which have been previously discussed in Chapter 2. In such cases a single channel placed over these muscles would register an EMG signal that is generated by either of them.

Table 4.1: Details on the different GA categories, the GAs and the grasps included.

GA Category	GA Name	Number of Grasps in GA	Grasps Included
All Grasps	All Grasps	15	T, I, M, R, L, T-I, T-M, T-R, T-L, I-M, M-R, R-L, I-M-R, M-R-L, HC
Single Grasp	Thumb	1	T
	Index	1	I
	Middle	1	M
	Ring	1	R
	Little	1	L
Focal Grasp	Thumb Focal	6	T, T-I, T-M, T-R, T-L, HC
	Index Focal	5	I, T-I, I-M, I-M-R, HC
	Middle Focal	7	M, T-M, I-M, M-R, I-M-R, M-R-L, HC
	Ring Focal	7	R, T-R, M-R, R-L, I-M-R, M-R-L, HC
	Little Focal	5	L, T-L, R-L, M-R-L, HC

The *Focal Grasp* category contains all GAs that were defined for containing any grasps that involved the use of the ‘focal finger’. The focus of these GAs was on the impact that the ‘focal finger’ would have on the selection process when it came to the optimal channel combination. In many cases the result for different GAs in this category were expected to be similar, since there were grasps that were common to multiple GAs. However, there were cases where a GA identified a different set of optimal channels, and these differences were investigated.

4.2 Generation of Channel Combinations

To find the best channel combination for the 2-channel, 3-channel and 4-channel setups, all possible combinations needed to be generated and compared. The limit on the number of channels in each respective setup lead to the maximum number of possible combinations indicated in Table 4.2. For example, for any GA, when analysing the GA to find the best 2-channel setup, there were a total of 28 combinations of the channels 1 to 8 that needed be generated and analysed against each other. These values are calculated using the binomial coefficient method, in this case $\binom{8}{2}$ = 28, $\binom{8}{3}$ = 56 and $\binom{8}{4}$ = 70. In total there were 154 (28 + 56 + 70) combinations generated across the three reduced-channel setups for a single GA.

Table 4.2: Number of possible combinations when using only two, three or four channels.

Number of Channels	Number of Combinations
2	28
3	56
4	70

The data used in this study was collected over a twenty-second time period [26], [32]. This total time was split into four smaller time periods (TPs): 0 – 5s, 5 – 10s, 10 – 15s and 15 – 20s. In addition to these smaller TPs, a full 0 – 20s TP was used as a comparison marker when it came to analysing the combinations. The splitting up of the TPs allowed for a more detailed analysis into how prevalent channel combinations change with time. Each combination thus consisted of a group of five TP sections.

In cases where a GA had multiple grasps associated with it, the relevant TPs from each grasp were appended together to form the full amount of data required for the analysis. For example, consider the Thumb Focal GA, which contained six grasps. When generating the 2-channel combinations for this GA, the 0 – 5s TP for the relevant channels for all six grasps were appended together, and this occurred in the same order for each TP.

Once the combinations and TPs were generated, there were a total of 770 (28*5 + 56*5 + 70*5) channel combinations for a single GA, spanning the 2-channel, 3-channel and 4-channel setups.

4.3 Error Calculation

In order to find which channel combination best represented the 2-channel, 3-channel and 4-channel setups, three error metrics: NRMSE, CC, and MSC were used, as reviewed in Chapter 2. These error metrics were applied to each of the individual TPs within each combination. This allowed for comparisons between similar TP's in different combinations.

The original eight channels of data for the GA were used to compute the error metrics. PCA was applied as an FEM, as described previously in Chapter 2. The use of PCA generated an eight-by-eight covariance matrix along with its eigenvalues and eigenvectors. The Eigenvectors are re-ordered according to the eigenvalues, such that the columns represent the eight PCs of the data, in order from highest to lowest variance values. A 2-PC model of the data was created by retaining only the first two PCs from the 8-PC model. This 2-PC model was reversed to give the reconstructed signals for the eight channels of data. Note that PCA was not used as a dimensionality reduction technique in this case.

The 2-PC model enabled a comparison between the eight original channels and eight reconstructed channels. Each channel of the 8-PC and 2-PC models was compared using the NRMSE, CC and MSC error metrics. These three values represent the correlation between the two models for each channel. To calculate the error metric values for a particular combination (which includes either two, three or four channels), the error values for all the channels included in the combination were averaged. This gave three error metrics that represented each combination. This process was performed for each of the TPs, so each channel combination had three error metrics that represent each of its five TPs.

The reason that the 8-PC model and the 2-PC model were compared to each other was due to signal variance bias. When a particular muscle contracts, the channel that is measuring that muscle has an increased amplitude. This can be seen in a PCA as a larger variance when compared to non-active channels. Performing PCA and retaining only the first two PCs meant that once the channel signals were reconstructed, the channels that were actively measuring contraction had lower error values (since PCA retains variance) which is equivalent to a larger amplitude. Thus, when comparing the 8-PC model with the 2-PC model using the error metrics, the active channels within the combination of channels were determined according to least overall error.

4.4 Error Analysis

For each of the three channel setups, all possible combinations were generated, each combination consisting of five TPs, and each TP being represented by three error metrics. These error metrics were compared to identify a single best channel combination for each of the 2-channel, 3-channel and 4-channel setups. This was done in two stages:

In the first stage the error metrics for the *same* TPs across combinations were compared, and a best channel combination was identified for each of the five TPs. This reduces the 770 (28*5 + 56*5 + 70*5) combinations to 15 (5 + 5 + 5). For example, in the 2-channel setup, the 28 combinations are compared on a TP-to-TP basis, and only a single channel combination is identified for each TP. The error metrics for the channel combinations were compared using the following rules:

1) The channel combination with the lowest NRMSE, highest CC and highest MSC was chosen from all the combinations.
2) This optimal channel combination's error metrics were compared to the average of all the error metrics to ensure that they are lower than the average, since if the best error values were not better than the total average, then there was a mistake in the selection of the optimal channel combination.
3) There were cases where the three error metrics did not all agree on what the optimal channel combination was. In these cases, the combination that

showed the best two out of the three metrics was selected as the optimal channel combination.

4) There were cases where none of the three error metrics agreed on what the optimal channel combination was. Since the three error metrics were given the same weight, such a result was completely inconclusive.

Upon completion of this process, each channel setup had five channel combinations (one for each TP), or in very rare cases there was no outcome.

In the second stage, all channel combinations within either the 2-channel, 3-channel or 4-channel setups, for the *different* TPs, were compared to each other. This identified the overall best combination through all the TPs, giving a single optimal channel combination for each of the 2-channel, 3-channel and 4-channel setups. In the majority of cases the channel combinations remained consistent throughout the different TPs, and were confirmed by the 0 – 20s TP. In cases where this did not occur however, a single optimal channel combination was identified. A sequence of steps was followed when comparing the optimal channel combinations from the different TPs to each other. This sequence was followed until an outcome was reached, and is as follows:

1) Considering all four of the TPs (excluding the 0-20s TP), select the most common channel combination.
2) If there is no clear optimal channel combination, include the 0-20 s TP as well.
3) If there is still no clear optimal channel combination, weight the combinations to favour those that were determined to be the optimal channel combination in their TP with confirmation of all three error metrics (as opposed to only two of the error metrics).
4) If there is still no clear optimal channel combination, choose the 0-20 s TP combination as the optimal channel combination.
5) If there is no 0-20 s TP optimal channel combination (due to being inconclusive), choose the combination that has the highest variance data content.

6) If all the TP combinations are inconclusive (none of them were confirmed by two or three error metrics), the channel combination is considered completely inconclusive, and this is indicated.

The sequences identified a single optimal channel combination for each of the 2-channel, 3-channel and 4-channel setups. It tended to show a progression of what channel was added when going from the 2-channel setup to the 3-channel setup for example.

This two-stage process was repeated for each GA, generating for each subject the table described at the beginning of Chapter 4 and seen in Chapter 6.

4.5 Chapter Summary

This chapter described the methodology for identifying the optimal channel combination for each GA, for the 2-channel, 3-channel and 4-channel setups. The described process yielded results for all eleven GAs for each subject.

Chapter 5 – Methods for Graphical Representation of Results

Chapter 4 focussed on identifying the optimal channel combinations for the 2-channel, 3-channel and 4-channel setups for each GA, for each subject to answer RA1-P1. This chapter discusses the methodology that could answer RA1-P2: How much impact does the reduction in the number of electrodes have on the variance content of the data? These results serve as a quality evaluation, where the reduced-channel setups can be compared directly to their baseline eight-channel setup counterparts.

This quantitative analysis employed the variance of PCA as a metric for the information content retained in the reduced-channel combinations. For each *All Grasps* optimal channel combination, the percentage of variance retained (PVR) by the reduced-channel setup was calculated. These percentages are presented in a graphical form in Chapter 6 that allows for comparison when different numbers of channels, as well as the different TPs are considered.

PCA employs variance to indicate which dimensions of a dataset are important, and this principle was applied to provide a measure indicating which channels are important: The PVR quantified the contribution that a channel had relative to the total amount of variance for all channels measured together.

The computation of the PVR metric is detailed in Section 5.1.

5.1 Percentage of Variance Retained (PVR)

As discussed in Chapter 4 PCA involves the generation of an eight-by-eight covariance matrix involving all the channels. This was done prior to identifying the PCs. For each GA a covariance matrix for all eight channels was calculated, denoted C. The trace of this covariance matrix sums all variances of all eight channels. This value is a baseline variance content using all the electrodes which can be compared to the reduced electrodes setup. The same procedure is followed to generate a covariance matrix for only the optimal reduced channel combinations, denoted *B. T*he trace of *B* reflects the total amount of variance when only using the optimal channels. A PVR is defined as the ratio between the two traces:

$$PVR = \frac{trace\ (B)}{trace\ (C)} x\ 100 \qquad (2)$$

This PVR calculation can be repeated for each TP within a channel combination, thus allowing for the different TPs to be compared. The patterns of these percentages were compared across different subjects, as well as between the *Single Grasp* GAs and the *Focal Grasp* GAs. These results are discussed in Chapter 7.

5.2 Chapter Summary

Additional results were generated to supplement the tables generated in Chapter 4 and presented in Chapter 6 to provide an answer for RA1-P2: How much impact does the reduction in the number of channels have on the variance content of the data?

Chapter 6 – Results

The results generated using the methodologies described in Chapter 4 and Chapter 5 are presented here. Each subject's results are in the form of: 1) A table that shows all optimal channel combinations for all the GAs that were investigated, for the 2-channel, 3-channel and 4-channel setups, and 2) A graph that shows the PVR for the *All Grasps* GA. These are displayed in Sections 6.1 to 6.7. Note that for each subject, only the most common optimal channel combinations are presented. This follows the process outlined in Section 4.4., whereby the five TPs for each GA were combined to get a single optimal channel combination.

Section 6.8 used the individual subject results to compile a table of the most common optimal channel combinations for each subject for the 2-channel, 3-channel and 4-channel setups. These compiled results are compared in discussion in Chapter 7.

Section 6.9 considers the averages of the PVRs for each subject across each of their TPs, which were visualised for further discussion in Chapter 7.

6.1 Subject 1

The results of the optimal channel combinations for Subject 1 are shown in Table 6.1, followed by the PVR results of the *All Grasps* GA for the 2-channel, 3-channel and 4-channel setups in Figure 6.1.

Table 6.1: Subject 1's optimal channel combinations for the GAs.

GA Analysed		Most Common Combination		
Name	**Grasp count**	**2-channel**	**3-channel**	**4-channel**
All	15	1 7	1 7 8	1 2 7 8
Thumb	1	1 6	1 5 6	1 5 6 8
Index Finger	1	1 6	1 2 6	1 2 6 8
Middle Finger	1	1 8	1 2 8	1 2 7 8
Ring Finger	1	1 5	1 2 5	1 2 5 8
Little Finger	1	1 4	1 4 5	1 4 5 8
Thumb Focal	6	1 7	1 7 8	1 2 7 8
Index Focal	5	1 7	1 7 8	1 2 7 8
Middle Focal	7	1 7	1 7 8	1 2 7 8
Ring Focal	7	5 7	5 6 7	5 6 7 8
Little Focal	5	1 7	1 7 8	1 2 7 8

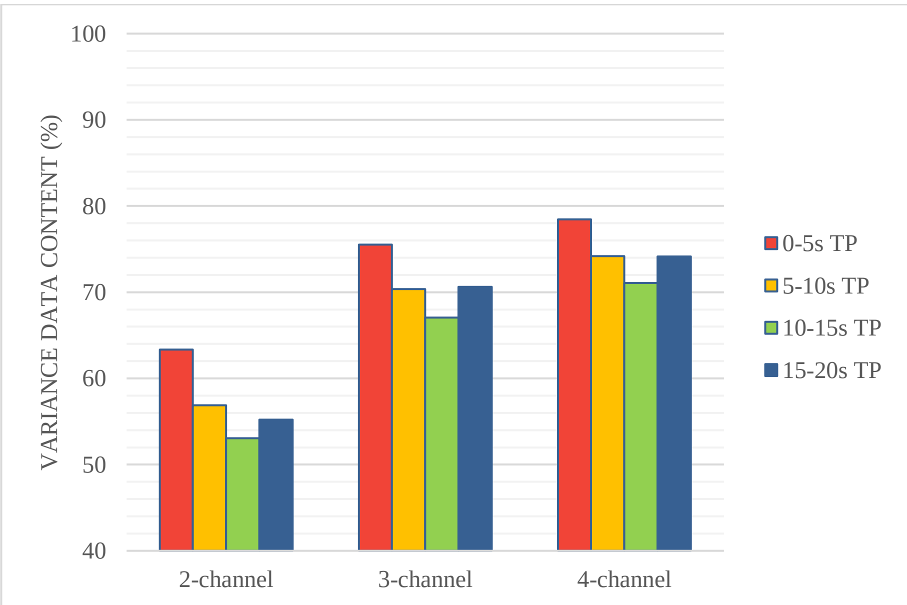

Figure 6.1: Subject 1's PVR for the *All Grasps* GA.

6.2 Subject 2

The results of the optimal channel combinations for Subject 2 are shown in Table 6.2, followed by the PVR of the *All Grasps* GA for the 2-channel, 3-channel and 4-channel setups in Figure 6.2.

Table 6.2: Subject 2's optimal channel combinations for the GAs.

GA Analysed		Most Common Combination		
Name	**Grasp count**	**2-channel**	**3-channel**	**4-channel**
All	15	5 8	4 5 8	3 4 5 8
Thumb	1	1 8	1 7 8	1 2 7 8
Index Finger	1	1 8	1 7 8	1 2 7 8
Middle Finger	1	1 8	1 2 8	1 2 7 8
Ring Finger	1	5 7	5 7 8	1 5 7 8
Little Finger	1	1 8	1 7 8	1 2 7 8
Thumb Focal	6	7 8	6 7 8	1 6 7 8
Index Focal	5	5 8	4 5 8	5 6 7 8
Middle Focal	7	5 8	1 5 8	None
Ring Focal	7	5 8	5 7 8	1 5 7 8
Little Focal	5	5 8	5 7 8	None

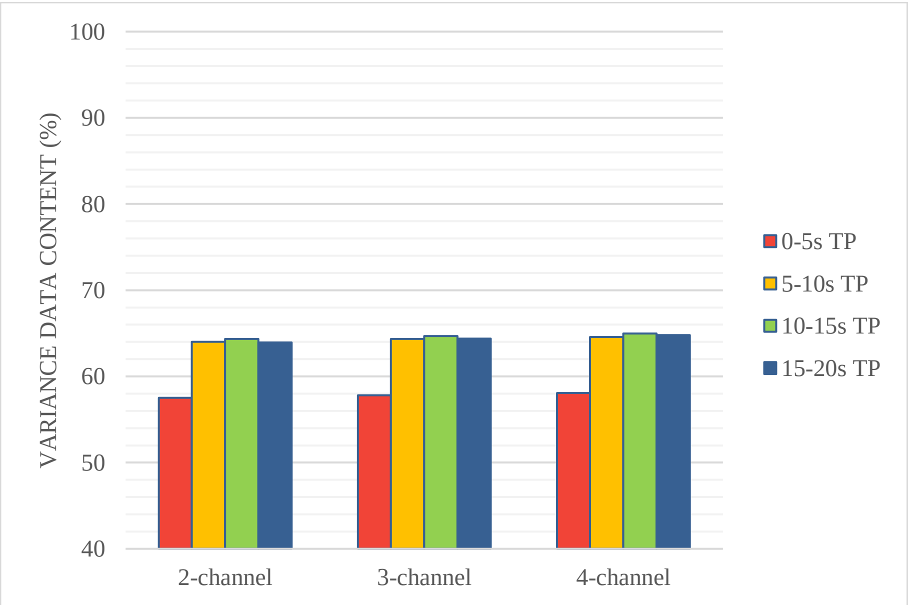

Figure 6.2: Subject 2's PVR for the *All Grasps* GA.

6.3 Subject 3

The results of the optimal channel combinations for Subject 3 are shown in Table 6.3, followed by the PVR results of the *All Grasps* GA for the 2-channel, 3-channel and 4-channel setups in Figure 6.3.

Table 6.3: Subject 3's optimal channel combinations for the GAs.

GA Analysed		Most Common Combination		
Name	**Grasp count**	**2-channel**	**3-channel**	**4-channel**
All	15	7 8	1 7 8	1 6 7 8
Thumb	1	1 8	1 2 8	1 2 7 8
Index Finger	1	1 8	1 7 8	1 6 7 8
Middle Finger	1	1 8	1 7 8	1 2 7 8
Ring Finger	1	1 6	1 6 8	1 2 6 8
Little Finger	1	1 8	1 2 8	1 2 7 8
Thumb Focal	6	7 8	1 7 8	1 6 7 8
Index Focal	5	7 8	1 7 8	1 6 7 8
Middle Focal	7	7 8	1 7 8	1 6 7 8
Ring Focal	7	7 8	1 7 8	1 6 7 8
Little Focal	5	7 8	1 7 8	1 6 7 8

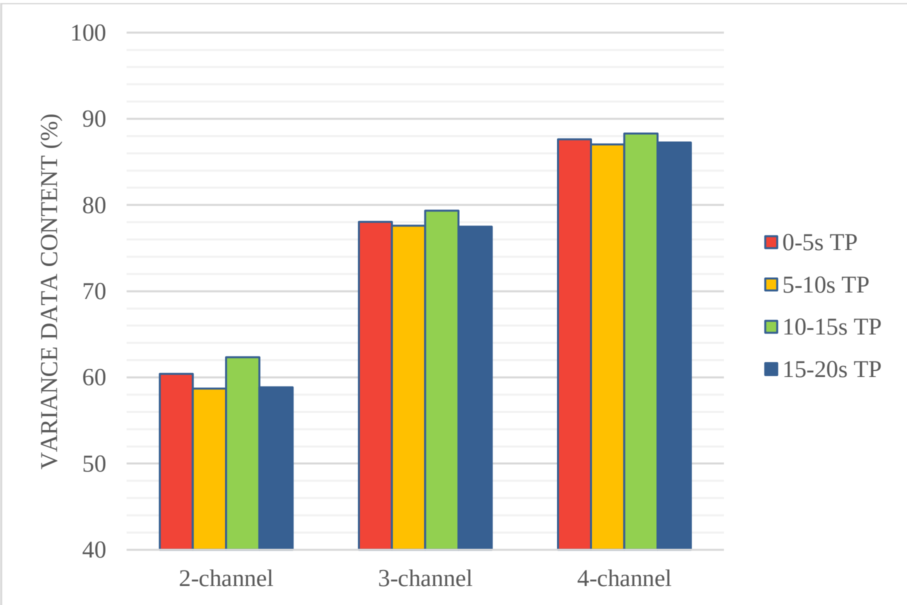

Figure 6.3: Subject 3's PVR for the *All Grasps* GA.

6.4 Subject 4

The results of the optimal channel combinations for Subject 4 are shown in Table 6.4, followed by the PVR results of the *All Grasps* GA for the 2-channel, 3-channel and 4-channel setups in Figure 6.4.

Table 6.4: Subject 4's optimal channel combinations for the GAs.

GA Analysed		Most Common Combination		
Name	**Grasp count**	**2-channel**	**3-channel**	**4-channel**
All	15	5 6	5 6 7	3 4 5 6
Thumb	1	5 6	3 5 6	1 2 6 8
Index Finger	1	5 6	4 5 6	4 5 6 7
Middle Finger	1	5 6	4 5 6	4 5 6 7
Ring Finger	1	5 6	5 6 7	4 5 6 7
Little Finger	1	5 6	1 5 6	1 4 5 6
Thumb Focal	6	1 7	1 7 8	1 2 7 8
Index Focal	5	6 7	5 6 7	4 5 6 7
Middle Focal	7	6 7	5 6 7	3 5 6 7
Ring Focal	7	6 7	5 6 7	None
Little Focal	5	6 7	5 6 7	5 6 7 8

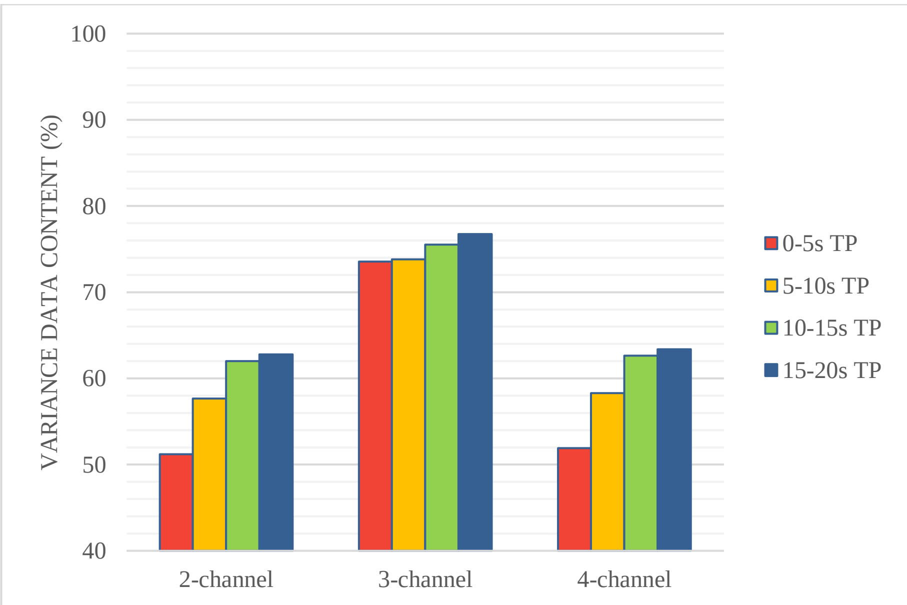

Figure 6.4: Subject 4's PVR for the *All Grasps* GA.

6.5 Subject 5

The results of the optimal channel combinations for Subject 5 are shown in Table 6.5, followed by the PVR results of the *All Grasps* GA for the 2-channel, 3-channel and 4-channel setups in Figure 6.5.

Table 6.5: Subject 5's optimal channel combinations for the GAs.

GA Analysed		Most Common Combination		
Name	**Grasp count**	**2-channel**	**3-channel**	**4-channel**
All	15	1 5	1 2 5	1 2 5 8
Thumb	1	1 6	1 5 6	1 5 6 8
Index Finger	1	1 6	1 2 6	1 2 4 6
Middle Finger	1	1 5	1 5 6	1 5 6 8
Ring Finger	1	1 5	1 5 6	1 2 5 6
Little Finger	1	1 6	1 5 6	1 2 5 6
Thumb Focal	6	1 5	1 2 5	1 2 5 8
Index Focal	5	1 5	1 2 5	1 2 4 5
Middle Focal	7	1 5	1 5 8	1 4 5 8
Ring Focal	7	1 5	1 5 8	1 2 5 8
Little Focal	5	1 5	1 2 5	1 2 5 8

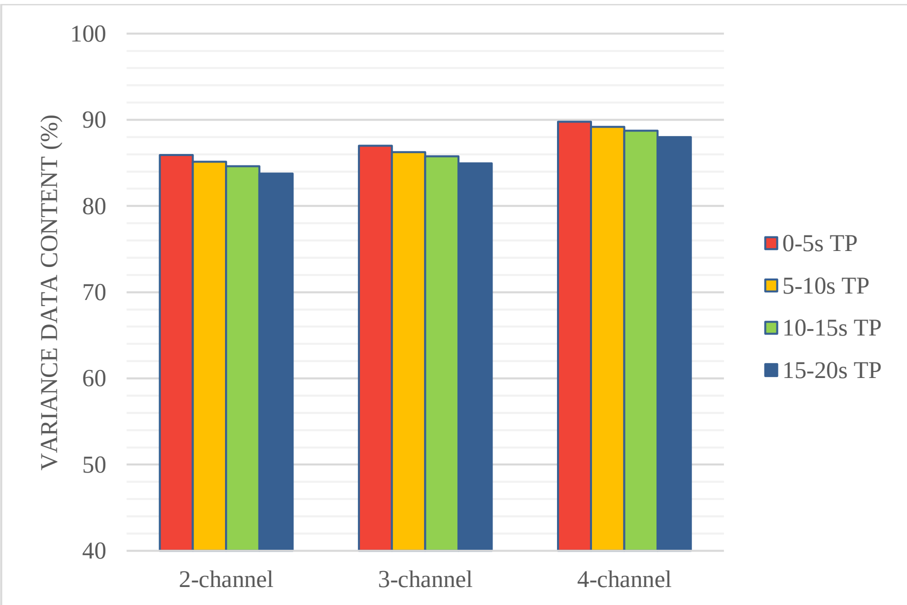

Figure 6.5: Subject 5's PVR for the *All Grasps* GA.

6.6 Subject 7

The results of the optimal channel combinations for Subject 7 are shown in Table 6.6, followed by the PVR results of the *All Grasps* GA for the 2-channel, 3-channel and 4-channel setups in Figure 6.6.

Table 6.6: Subject 7's optimal channel combinations for the GAs.

GA Analysed		Most Common Combination		
Name	**Grasp count**	**2-channel**	**3-channel**	**4-channel**
All	15	1 5	1 2 5	1 2 5 8
Thumb	1	1 8	1 7 8	1 2 7 8
Index Finger	1	1 8	1 7 8	1 2 7 8
Middle Finger	1	1 8	1 2 8	1 2 7 8
Ring Finger	1	5 8	1 5 8	1 5 7 8
Little Finger	1	1 5	1 2 5	1 2 5 6
Thumb Focal	6	1 5	1 2 5	1 2 5 8
Index Focal	5	1 5	1 5 8	1 2 5 8
Middle Focal	7	5 7	5 7 8	1 5 7 8
Ring Focal	7	5 7	5 7 8	5 6 7 8
Little Focal	5	5 7	5 7 8	1 5 7 8

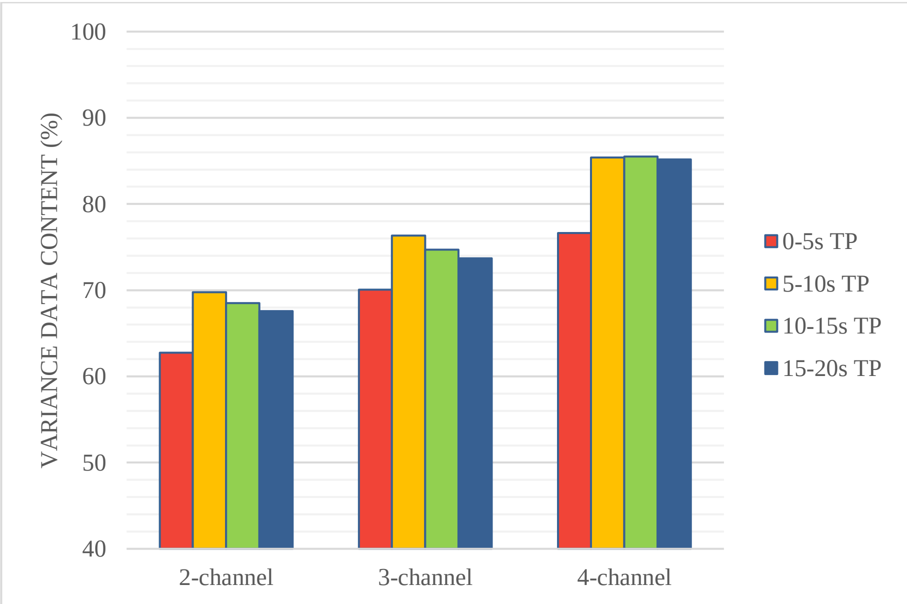

Figure 6.6: Subject 7's PVR for the *All Grasps* GA.

6.7 Subject 8

The results of the optimal channel combinations for Subject 8 are shown in Table 6.7, followed by the PVR results of the *All Grasps* GA for the 2-channel, 3-channel and 4-channel setups in Figure 6.7.

Table 6.7: Subject 8's optimal channel combinations for the GAs.

GA Analysed		Most Common Combination		
Name	**Grasp count**	**2-channel**	**3-channel**	**4-channel**
All	15	1 5	1 5 6	1 5 6 7
Thumb	1	1 2	1 2 8	1 2 3 8
Index Finger	1	1 8	1 7 8	1 2 7 8
Middle Finger	1	1 2	1 2 3	1 2 3 8
Ring Finger	1	1 5	1 5 6	1 2 5 6
Little Finger	1	1 2	1 2 8	1 2 3 8
Thumb Focal	6	1 5	1 5 6	1 5 6 7
Index Focal	5	1 6	1 6 7	1 5 6 7
Middle Focal	7	1 6	1 5 6	1 5 6 7
Ring Focal	7	5 8	5 6 8	5 6 7 8
Little Focal	5	1 5	1 5 6	1 5 6 7

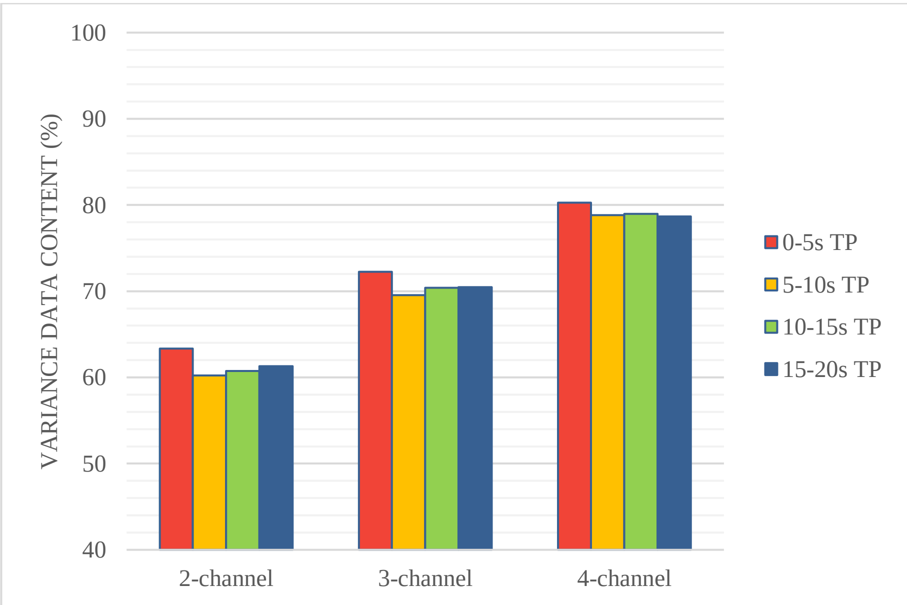

Figure 6.7: Subject 8's PVR for the *All Grasps* GA.

6.8 Most Common Channel Combinations

The overall most common channel combinations for the 2-channel, 3-channel and 4-channel setups for each subject are presented in Table 6.8.

In identifying the most common channel combinations for each subject, the results for the GAs were weighted. The *All Grasps* GA was given a weighting of value three, the *Focal Grasp* GAs were each given a weighting of value two, and the *Single Grasp* GAs were each given a weighting value of one. These weightings were assigned according to the number of grasps in the GAs; the *All Grasps* GA has 15 grasps, the *Focal Grasp* GAs have between five and seven grasps, and the *Single Grasp* GAs have a single grasp each.

This was done to give more weight to the GAs that included more grasps, since these GAs found optimal channel combinations under more complex circumstances (the inclusion of multiple grasps into the analysis as opposed to a single grasp). It is noted that each of the *Focal Grasp* and *Single Grasp* GA categories have five GAs each; and the *All Grasps* GA only has one. The score for the *All Groups* GA was kept at three to avoid over-fitting the optimal channel combination to a single result.

Table 6.8: Overall most common channels for each subject for the 2-channel, 3-channel and 4-channel setups.

Subject Number	Most common channel combinations		
	2-channel setup	3-channel setup	4-channel setup
1	1 7	1 7 8	1 2 7 8
2	5 8	5 7 8	1 2 7 8
3	7 8	1 7 8	1 6 7 8
4	5 6	5 6 7	4 5 6 7
5	1 5	1 2 5	1 2 5 8
7	1 5	1 2 5	1 2 5 8
8	1 5	1 5 6	1 5 6 7

The optimal channel combination for each reduced-channel setup with the highest score was identified and presented. This analysis did not yield any pattern for 3 out of the 231 (33*7) results, a total of 1.3%, which were not considered further in this study.

6.9 Average Percentage Variance Retained

As described in Chapter 5 the results for the PVRs for each TP were calculated using the identified optimal channel combinations for the *All Grasps* GA for each subject. These results were displayed in a graph for each subject, showing the progression of TPs. Table 6.9 displays the average PVR of all TPs for each channel setup for each subject. These results are presented graphically in Figure 6.8.

Table 6.9: PVR by each subject for the All Grasps optimal channel combinations, for the 2-channel, 3-channel and 4-channel setups.

Subject	Variance Data Content (%)		
	2-channel setup	3-channel setup	4-channel setup
1	57.1	70.9	74.5
2	62.5	62.8	63.1
3	60.1	78.1	87.5
4	58.4	74.9	59.1
5	84.9	86.0	88.9
7	67.2	73.7	83.2
8	61.4	70.7	79.2

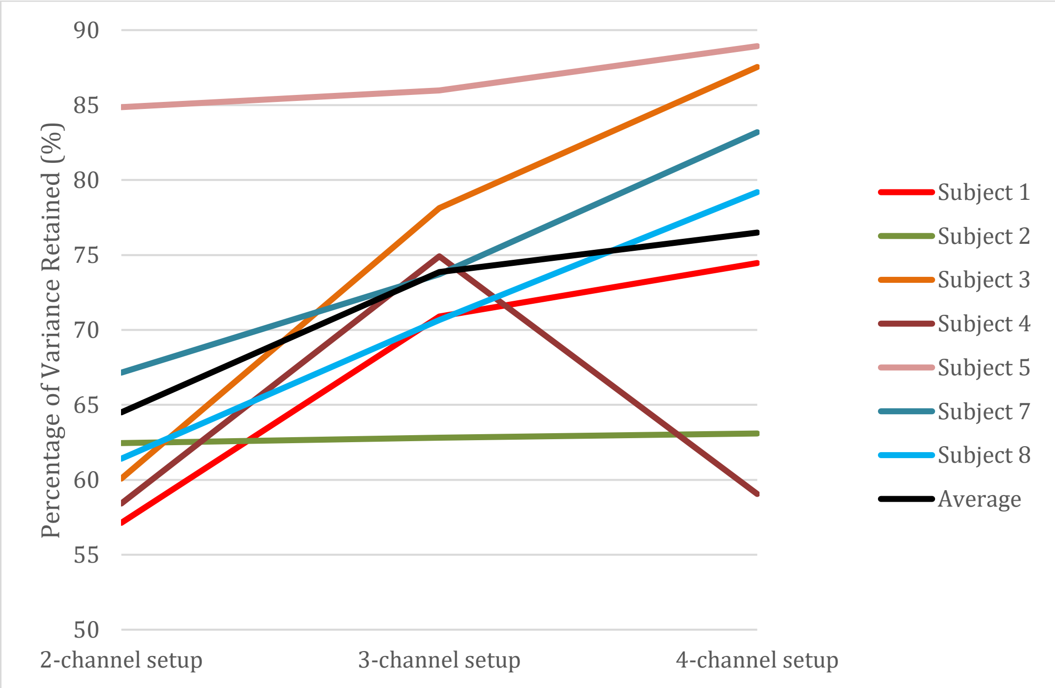

Figure 6.8: Average PVR for each subject for each channel combination (coloured lines), including the average for all subjects (black line).

6.10 Chapter Summary

This chapter presented the results obtained using the methods described in Chapter 4 and Chapter 5. Results for each of the seven subjects were presented and were followed by results summarising the overall most common optimal channel combinations, as well as the average PVR, across all subjects. The main findings of this study could be better observed and discussed by looking at the results across all subjects, as opposed to on a subject-by-subject basis. These latter results will be discussed in Chapter 7.

Chapter 7 – Discussion

This chapter discusses the derived results presented Table 6.8, Table 6.9 and Figure 6.8, in Chapter 6. The insights gained from these results are presented, with the aim of using them to answer the RQ.

Section 7.1 covers the proposed EMG electrode placement and muscle associations that the current study uses as a basis for discussion. These were based on the study where the data was originally collected by Khushaba and Kodagoda [26], and the proposed placements by Naik *et al.* [61] discussed in Chapter 3.

Section 7.2 discusses the optimal channel combinations for the 2-channel setup. Following this, the 3-channel setup is discussed in Section 7.3, and lastly the 4-channel setup is discussed in Section 7.4. A number of conclusions are made in each section. These were used to answer RQ and related research goals.

Section 7.5 discusses the PVR trends and identifies some important results that are used to help answer the RQ and associated research goals.

Lastly, Section 7.6 combines the discussions and results of the previous sections to answer the RQ proposed in Chapter 1. This is done through systematically dealing with each goal: RA1-P1, RA1-P2, RA1 and RA2 and their relations to each other.

7.1 Updated Electrode Placements on the Forearm

The proposed electrode placements used in this study were based on the electrode placement proposed by Naik *et al.* [61], which were themselves based on the placements in the Khushaba and Kodagoda [26]. These placements were marked on anatomical diagrams from Chapter 2 such that the association between the electrodes and muscles can be identified, as shown in Figure 7.1, Figure 7.2 and Figure 7.3. Following this, the active underlying muscles (if they are below the surface muscles) are identified and their associations mapped, as shown in Table 7.1.

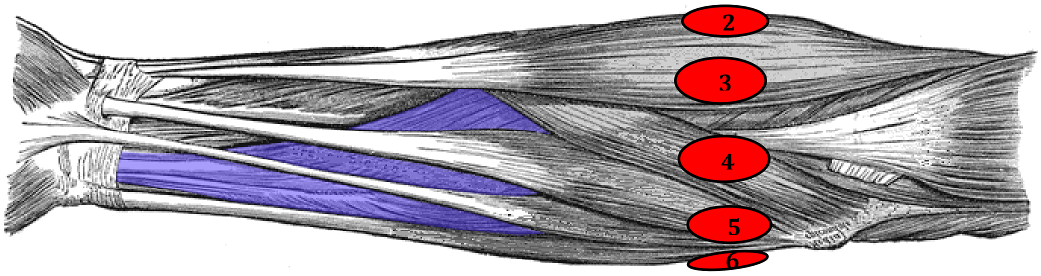

Figure 7.1: Anterior surface view of the right forearm, showing the electrode placements (numbered red circles) and FDS (blue) (Adapted from [58]).

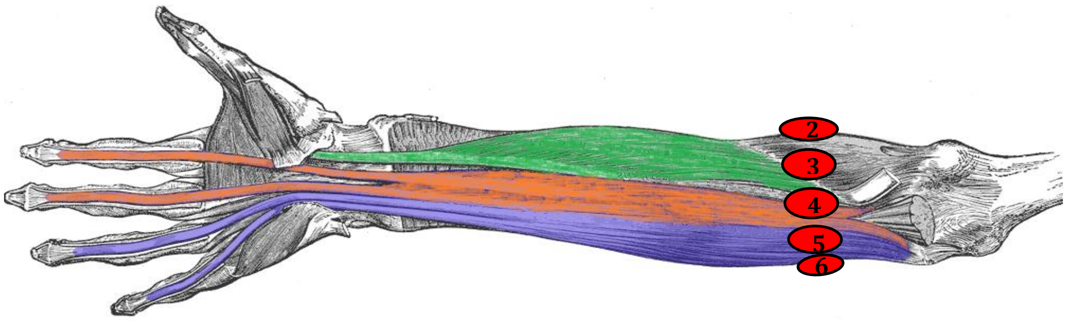

Figure 7.2: Anterior deep view of the right forearm, showing the same electrode placements as in Figure 7.1 (numbered red circles). Seen here are the FPL (green), FDP-L (orange) and FDP-M (blue) (Adapted from [59]).

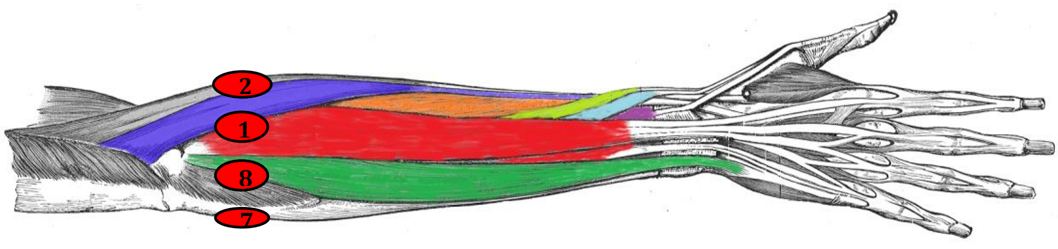

Figure 7.3: Posterior surface view of the right forearm, showing the electrodes placements (numbered red circles). Seen here are ECRL (blue), ED (red), ECU (green), ECRB (orange), EPL (purple), APL (light green) and EPB (light blue) (Adapted from [60]).

Table 7.1: Muscle-electrode associations used in the current study, including the deeper active muscles.

Surface Muscle	Electrode(s)	Active Muscles (might be deeper to the surface muscle)
ED	1	ED
Brachioradialis	2, 3	FPL
Supinator	4	FDS, FPL, FDP-L
FCR	5	FDS, FDP-L, FDP-M
FCU	6, 7	FDP-M
ECU	8	ECU

These associations assist the discussion on the results of Chapter 6 with respect to the optimal electrode placements that were identified, and the associated muscles involved. Although the exact placement of the electrodes in the original Khushaba and Kodagoda study could not be verified [26], the current study provides correspondence between EMG electrodes and muscles which may give some indication on the relative importance of the various muscles in the grasps. This avoids the traditional assumption that an electrode placed directly over a specific muscle will always yield and acceptable-quality EMG signal.

The region near electrodes 5, 6 and 7 is commonly referred to as the common flexor tendon, where some of the anterior surface muscles, including non-marked muscles FCR and FCU attach. Although these muscles are not directly involved in the hand grasps as discussed in Chapter 2, the common attachment at the common flexor tendon may in some cases cause electrodes 6 and 7 to record additional EMG signals that may be generated by other muscles.

Additionally, Naik *et al.* [61] consider electrodes 1, 2, 7 and 8 to be located on the posterior aspect of the forearm, with electrodes 3, 4, 5 and 6 on the anterior aspect. The current study proposes that electrode 7 is a part of the anterior electrodes, where only electrodes 1, 2 and 8 are located posteriorly, and electrodes 3, 4, 5, 6 and 7 are located anteriorly. Even though channel 2 is a posterior channel, its unique location means that it might still be activated when the thumb is flexed, which requires the FPL muscle.

7.2 2-Channel Setup Trends

When considering the 2-channel setup in Table 6.8, it becomes clear that there is a posterior channel and an anterior channel for each subject, except for Subject 4, where there are two anterior channels present. The deviation from the trend for Subject 4 will be addressed at multiple points in the discussions to follow.

In terms of the posterior channels, channels 1 and 8 correspond to the ED and ECU muscles respectively. The presence of these channels in the optimal combinations could initially be questioned, since the grasps under investigation are only concerned with finger flexion, not extension. However, the inclusion of these channels can be explained by the positioning of the non-active fingers when a single or group of fingers is flexed. The grasp images in Chapter 3 show that when performing any grasp, the non-active fingers are not relaxed, but are rather extended to be held straight. The extension is achieved by activating the ED muscle, hence the inclusion of channel 1.

Channel 8 is located next to channel 1 on the posterior forearm. It is normally associated with the ECU muscle as seen in Figure 7.3. The ECU muscle should only be active when all the fingers are closed together (as indicated in Table 2.1), so would not be considered very commonly active. There are two possible reasons why channel 8 is seen actively: 1) The nature of EMG electrode placements (because of differences in the anatomy of subjects) can cause electrodes to be shifted from their noted positions. In this case, channel 8 is measuring the activity of the ED muscle, not the ECU muscle. 2) The EMG signals measured by the electrodes is often a combination of EMG generated by multiple different muscles, not only the muscle the electrode is placed over. In this case, channel 8 may be placed correctly, but is still measuring the cross-talk from the ED muscle due to its proximity.

The anterior channels in the 2-channel setup are channels 5, 6 and 7. These channels correspond to the FDS, FDP-L and FDP-M muscles. Their presence is expected, since the muscles correspond directly to the flexion of the fingers, and these muscles are associated with the common flexor tendon, where these muscles are attached.

The 2-channel combination of Subject 4 has a different pattern compared to the other subjects. In this case channels 5 and 6 are present, corresponding to the FDS and FDP muscles. The presence of these channels is not surprising. The lack of presence of any posterior channels could to be due to a lack of co-contraction by the ED muscle of this subject during testing. This presents an issue, since an optimal channel selection needs to account for the flexion of the fingers during contraction, as well as the extension of the fingers to return the hand to rest.

There are a few conclusions that can be drawn from the 2-channel setup. Firstly, the combinations for each subject consist of an anterior channel (channel 5, 6 or 7) and a posterior channel (channel 1 or 8), except in Subject 4's case. Due to this, the channels for the subjects generally tend to be on opposite sides of the forearm to maximise EMG data collection. This is not the case for Subject 4, since channels 5 and 6 are directly next to each other on the anterior side of the forearm. Secondly, posterior channels 1 (over ED) and 8 (over ECU) are confirmed as important by Khushaba and Kodagoda [26], as well as Naik *et al.* [61]. Khushaba and Kodagoda [26] generally suggest that these muscles may be relevant, and Naik *et al.* [61] specifically discusses the importance of ED and ECU as a part of their *Simple Finger Movements* results.

7.3 3-Channel Setup Trends

The 3-channel setups from Table 6.8 follow on from the 2-channel setups. For each subject, an additional channel is added to the channels presented in the 2-channel setup. This progression is important to note, since if channels are identified as important for the strictest optimisation process (2-channel setup), then they should appear in the 3-channel and 4-channel setups.

The channel added from the 2-channel to 3-channel setup is not the same for each subject. Although the subjects are consistent in terms of adding a channel to the channels seen in the 2-channel setup, these additional channels are not the same for each subject. This indicates that there is some inter-subject variance, which is expected for an optimisation process such as this, since the subjects' all have differing muscle profiles.

The exact combinations in the 3-channel setups might be different across subjects, but trends can still be identified. With the addition of a third channel, some identifiable subject sub-groups can be seen. Subjects 1, 2 and 3 show a disposition towards including channels 7 and 8, with some variation on the third channel (denoted group 1). Subjects 5, 7 and 8 select for channels 1 and 5, again with some variation on the third channel (denoted group 2). Note the presence of a posterior channel and an anterior channel when identifying these sub-groups. Subject 4 continues to show a deviation from the other subjects when considering the 3-channel setup. Even though this is the case, Subject 4 remains consistent in the addition of a channel (channel 7) to the channels present in the 2-channel setup (channels 5 and 6), but this additional channel is also an anterior channel. This further supported the idea that there was no finger extension during testing.

An additional posterior channel was added for Subjects 1, 3, 5 and 7. Channel 2 is the new type of channel that is seen in the 3-channel setup, and its unique location (lying over FPL) indicates that its inclusion is due to the flexion actions of the thumb.

An additional anterior channel was added for Subjects 2, 4 and 8. The anterior channels show more consistency than the posterior channels in terms of location. All the anterior channels (channels 5, 6 and 7) are located around the common flexor tendon, corresponding to the FDS, FDP-L and FDP-M muscles. This indicates that the grasps that tend to give a higher EMG reading are those were multiple muscles are involved at the same time.

When Andrews [41] and Andrews *et al.* [17] considered a multiple-finger typing task, the FDP and ED muscles are identified as being most commonly selected for when using two channels. Extending this result to four channels showed selection for electrode placements over FDS, FDP, ED and ECU. In the current study channels 5, 6 (and 7), 1 and 8 correspond to these muscles.

7.4 4-Channel Setup Trends

The 4-channel setups from Table 6.8 follow on from the 3-channel setups. As discussed previously, an additional optimal channel is added to the previously optimally-selected channels in the 3-channel setup. This occurs in all subjects except Subject 2, where channels 1 and 2 are added, and channel 5 is removed from the combination.

As before, the inter-subject variation is evidenced by the difference in optimal channel combinations for the different subjects. The two subject sub-groups identified previously in Section 7.3, namely group 1 (channels 7, 8 and a variable channel)) and group 2 (channel 1, 5 and a variable channel) can be extended to include an additional channel. Channel 1 can be added group 1, so it includes channels 1, 7, 8 and a variable fourth channel. Channel 2 can be added to group 2, so it includes channels 1, 2, 5 and a variable fourth channel.

Similarly to the previous case, there is variation on the fourth channel within the sub-groups. The sub-groups display some interesting trends, even though overall the channel combinations are converging. The electrodes for group 1 (channels 1, 7 and 8) are all located in a focussed area on the forearm. This contrasts the placements of the electrodes for group 2 (channels 1, 2 and 5), where the electrodes are placed in a dispersed fashion. This indicates that there is no particular pattern to the groupings of channels.

As channels have been added, in terms of posterior channels channel 2 has become much more common. Its unique location influences the inclusion of it. It is interesting to note that there are many GAs that include some form of thumb grasp (whether multiple-finger or single-finger). Due to this, it was expected that channel 2 would become more common in either the 2-channel or 3-channel setups. However, as evidenced, the contributions from the other GAs outweighed channel 2 until the 4-channel setup. This is potentially due to the combined contraction strength of the other fingers that was stronger than the thumb. This meant that the optimal channels selected for were focussed around these muscles.

Subject 4 is an outlier for the 4-channel setup as well, when comparing their channel combinations to the other subjects. As mentioned previously, the possible reason for this could be a lack of co-contraction of non-active fingers during the EMG data collection process. However, only identifying anterior optimal channels in only one subject might indicate a form of data corruption that was not identified during the visual screening process.

When considering the 2-channel, 3-channel and 4-channel setups together, some of the more notable channels are 1, 2, 5, 6, 7 and 8. These are shown in Figure 7.4, Figure 7.5 and Figure 7.6. These notable channels correspond to the following active muscles: ED, FPL, FDS/FDP-L/FDP-M (common flexor tendon), and ECU. Channel 2 was a notable inclusion, for the fact that it was not relevant in the 2-channel context and not as commonly seen as the other channels in the 3-channel setup. Its inclusion is crucial, since it accounts for the flexion activity of the thumb.

As previously mentioned, some of these muscles were also identified as important by the dataset authors, Khushaba and Kodagoda [26]. Their conclusions were that the surface muscles ED, ECU, and FCU (which lies over the active muscle FDP) were relevant, even though their conclusions about what these muscles represent was somewhat limited in scope.

These differences in optimal channel combinations mean that the process of identifying optimal electrode placements is heavily subject-dependent. This is similar to a finding by Andrews *et al.* [17]. The important channels identified in this study can most certainly reduce the number of EMG electrode placements required. However, in some cases these electrode placements should be considered a preliminary starting point. Should the EMG data not be of sufficient quality, further testing of electrode placements may be necessary.

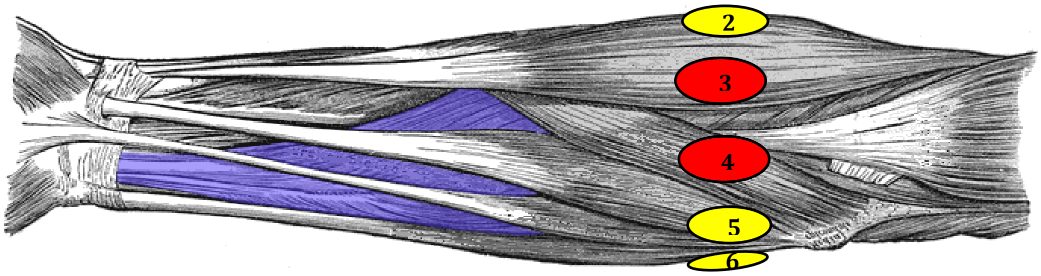

Figure 7.4: Anterior deep view of the right forearm, highlighting the notable channels in yellow (Adapted from [59]).

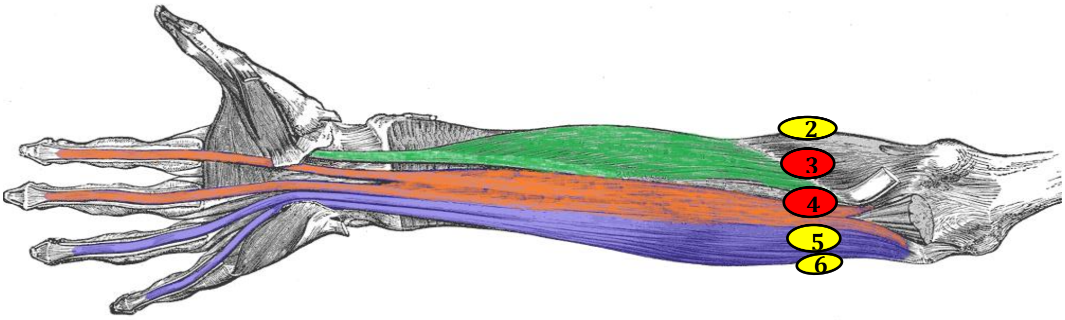

Figure 7.5: Anterior surface view of the right forearm, highlighting the notable channels in yellow (Adapted from [58]).

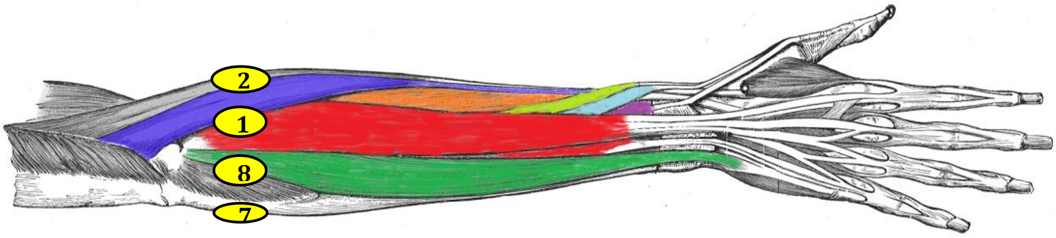

Figure 7.6: Posterior surface view of the right forearm, highlighting the notable channels in yellow (Adapted from [60]).

7.5 Percentage Variance Retained Trends

The average PVR for each subject for the 2-channel, 3-channel and 4-channel setups increase as the number of available channels increased, as illustrated in Table 6.9 and in Figure 6.8. This can be expected since more information is available for processing as the number of channels increase. Subject 4 was the exception to this rule, where the average PVR in the 4-channel setup was lower than the 3-channel setup. This could potentially be due to the selection of only anterior channels for the optimal 2-channel, 3-channel and 4-channel combinations.

Subject 5 displayed the highest consistent PVR for all the channel setups. In this case, the reduction in the number of channels to two still yielded a PVR of 84.9%. Subject 3 had the most significant change in PVR, increasing from 60.1% in the 2-channel setup to 87.5% in the 4-channel setup. There doesn't appear to be any correlation between the optimal channels in the 2-channel, 3-channel and 4-channel setups for these two well-performing subjects. Subject 3 was part of group 1 in terms of channel sub-groups, and Subject 5 was part of group 2. Even if a connection cannot be found between these sub-groups, it can be concluded that neither sub-grouping of channels is superior to the other. Thus, the problem of EMG electrode placement remains a subject-dependent task.

Subjects 2 and 4 showed unique results in terms of their PVR values. Subject 2's PVR was similar for all combinations at 62.5% for the 2-channel, 62.8% for the 3-channel and 63.1% for the 4-channel setups. Subject 4's PVR curve didn't increase from the 3-channel setup to the 4-channel setup, but rather decreased sharply. The potential reasons for these outlier cases can be attributed to the different patterns in the channel combinations for these subjects. In Subject 2's case, the loss of channel 5 in the 4-channel setup indicates that the channel combinations for the GAs were not converging. In Subject 4's case, the lack of a posterior channel present in the 4-channel setup could be the reason that the PVR was lower than in the 3-channel setup. It is not known why this is the case.

Apart from these two subjects, the PVR results support the assumption that this dataset can be optimised for a reduced number of electrodes. For the seven subjects used in this study, the minimum 2-channel setup PVR was 57.1% (Subject 1). The minimum 3-channel setup PVR was 62.8% (Subject 2), and the minimum 4-channel setup PVR was 59.1% (Subject 4). If the results for Subjects 2 and 4 are omitted due to their deviation from the trends, the minimum 2-channel setup PVR was 57.1% (Subject 1), the minimum 3-channel PVR was 70.7% (Subject 8) and the minimum 4-channel setup PVR was 74.5% (Subject 1).

7.6 Answering the Research Question

As described in Chapter 1 this study was segmented into various components. Each component will repeat the relevant question then answer the component. To answer the RQ, the components are answered in the following order: RA1-P1, RA1-P2, RA1, RA2, and finally the RQ.

Research Aim 1 – Part 1

What are the optimal channel combination trends that can be identified within and across subjects? Table 6.8 presents the most common optimal channel combinations for each subject. In addition to the individual trends noted for each subject, overall the most common channels are channels 1, 2, 5, 6, 7 and 8.

Research Aim 1 – Part 2

How much impact does the reduction in the number of electrodes have on the variance content of the data? Table 6.9 and Figure 6.8 show the impact of using limited numbers of EMG electrodes to collect data. With the minimum number of channels considered in this study (2-channel setup), the minimum PVR was 57.1%. The PVR improved to a minimum of 74.5% in the 4-channel setup, excluding the results of the problematic Subjects 2 and 4.

Research Aim 1

What are the optimal two, three and four channel combinations for each subject within the dataset, and how good is it compared to the original eight-channel dataset for each subject? This component of the study is answered by RA1-P1 and RA1-P2.

Research Aim 2

Given the two, three and four channel optimal combinations identified in RA1, which muscles are mainly responsible for generating this EMG data? Overall the most common channels are channels 1, 2, 5, 6, 7 and 8. The channels correspond to the following active muscles: ED, FPL, FDS, FDP-L, FDP-M (which make up the common flexor tendon), and ECU.

Research Question

In using an eight-channel EMG dataset, what are the optimal combinations of two, three and four EMG channels that consider the reduction in number of electrodes and their variance data content when compared to the original eight-channel dataset? As discussed previously, the optimal channel combinations for each subject vary, but overall the most common channels have been identified for the 2-channel, 3-channel and 4-channel setups for each subject, as well as the overall dominant channels being channels 1, 2, 5, 6, 7, and 8. The use of the optimal channel combinations for each subject gives a 2-channel PVR range of 57.1 – 84.9% a 3-channel PVR range of 70.7 – 86.0% and a 4-channel PVR range of 74.5 – 88.9%, when omitting the results for Subjects 2 and 4.

7.7 Future Work

The current study developed an algorithm that worked on the data that was used. This implies that it will work on future datasets of a similar format as well. An algorithm was developed as a proof-of-concept, but additional work needs to be done to further develop and validate the algorithm. Discussed here are a number of aspects that would benefit from additional work.

Future datasets that use the algorithm could benefit from using more electrodes (for example 16 electrodes). These 16 electrodes could be set up in different configurations, either in a single band around the forearm, or multiple bands at different levels of the forearm. This effectively gives the algorithm more data to work with to find optimal channel combinations.

Additional movements can also be added to the dataset, such as wrist movements. Previous work by Eisenberg *et al.* [62] identified that EMG data generated by wrist movements can be similar EMG generated by finger movements, and it would be important to be able to differentiate between the wrist and finger movements.

This study focussed on the amount of PVR that was maintained by the optimal channel combinations, but an aspect of PVR that would need to be investigated in future would be the threshold amount of PVR that is considered to be acceptable.

This would be very dependent on the context of the application. In general, once classification algorithms reach accuracies of more than 75% they start being considered “useful”. The same could apply to the PVR in this study. It would require substantial additional work to be able to conclude at what PVR there is enough data variance for use in further processing, such as training classification algorithms.

Lastly, the three error metrics (NRMSE, CC, and MSC) used to identify the optimal channel combinations were given an equal weighting when it came to using them to identify optimal channel combinations. Future work would involve identifying which of these metrics may be more important or relevant than the others; or which other error metrics could be used to better find optimal channel combinations.

7.8 Chapter Summary

This chapter aimed to answer the research goals of the RQ identified in Chapter 1. This was done using discussion into the results presented in Chapter 6 and there were some important insights that were gained in the process of answering these research goals, as well as the RQ.

The 2-channel, 3-channel and 4-channel setups were discussed, and each provided more insight into the trends that were shown in the results. For instance, the common presence of channel 1 (located on the ED muscle) in optimal channel combinations revealed that the extension of the fingers not actively involved in the grasps was noticeable. This is important when it comes to collecting the EMG data, and this should be accounted for when placing electrodes.

Given the insights gained, it was concluded that the subjects do show different optimal channel combinations due to inter-subject variability, but channels 1, 2, 5, 6, 7 and 8 were the common across the subjects. These channels correspond approximately to the ED, FDS, FDP and ECU muscles.

The PVR when using only select channels was discussed, and it was identified that the PVR improved with the increase in number of electrodes. The reduction in number of channels showed that a minimum PVR of more than 57% was seen when using a 2-channel setup, more than 62% when using the 3-channel setup, and more than 74% when using the 4-channel setup. These results do not include the PVRs for Subjects 2 and 4, since their PVRs did not follow the trends identified.

These results and discussions were used to directly answer each of the identified research goals, which were combined to answer the RQ proposed in Chapter 1.

Lastly, aspects of the study that are important to further explore in future work were identified and discussed. These aspects were outside of the scope of the current work, but are important to address.

Chapter 8 – Conclusion

This chapter summarises the study, briefly covering the main points for each chapter and their context with relation to the study goals.

Chapter 1 identified the need for trans-radial amputees to be able to perform their ADLs using a prosthetic hand, where such a hand is controlled using EMG. To effectively control a prosthetic hand using EMG, the placement and number of electrodes needs to be optimised. Often this is done using the classification accuracy of a classification algorithm as a metric for success, but this requires investigation into the correct use of the classification algorithm as well. A requirement to optimise the placement and number of EMG electrodes was identified, where the solution doesn't require a classification algorithm to be successful. To this end, an RQ was identified, and split into a series of research goals. These focussed on the optimal placement and number of EMG electrodes and the effects thereof when using these optimal placements in a limited-channel context.

Chapter 2 considered the research on the optimisation of EMG electrodes on the forearm, either by reducing the number of electrodes, or finding the best electrode placements. All these studies make use of classification accuracy as the metric for success. PCA is a method used to reduce the number of dimensions for classification systems, but can also be used to reduce the dimensionality and subsequently the quality of the data and compare the reduced-dimension model to the original data. The reduced-dimension model can be used to identify important EMG electrodes without the use of classification algorithms. To compare the reduced model and the original data, three error metrics are defined: NRMSE, CC and MSC. Additionally, the musculature of the forearm was reviewed in order to derive optimal electrode placements.

Chapter 3 describes an 8-channel EMG dataset that was ideal for use in this study. The subjects, hardware, software and testing procedures were outlined. This dataset consisted of eight subjects. Each subject performed a series of fifteen grasps with different combinations of fingers, and the EMG data was recorded using eight EMG electrodes arranged around the forearm. Validations were performed to ensure the quality of the dataset and note its limitations, as well as additional validations to ensure that Matlab's built-in PCARES function performed as expected.

Chapter 4 outlined the methodology to generate results that were used to answer part of the research objectives. It discusses generating all possible combinations of two, three and four channels of the original 8-channel EMG dataset. These combinations are compared to the original 8-channel dataset using PCA. The combination that showed the smallest error was identified as the optimal channel combination for that number of electrodes. This process was repeated for each subject for each of the defined GAs, to find an optimal channel combination for each GA. These results were tabulated for each subject.

Chapter 5 complemented Chapter 4, using the optimal channel combinations identified to find the variance data content that was retained from the original data to see what impact the reduction in EMG electrodes had on the amount of variance in the data. These results were shown in graphical format for each subject.

Chapter 6 presents the results generated in Chapter 4 and Chapter 5 for each subject. These results are compiled for simpler discussion in Chapter 7.

Chapter 7 discusses the results obtained with a focus on the optimal channel combinations for the 2-channel, 3-channel and 4-channel setups for the subjects. The discussion identified channels 1, 2, 5, 6, 7 and 8 as being important in the current study, which correspond approximately to the ED, FPL, FDS, FDP-L, FDP-M and ECU muscles. The impact of reducing the number of EMG electrodes was discussed, and it was seen that even when only using two of the channels, the PVR was more than 57%. These results provided answers to the multiple research goals, which led to answering the RQ in full. Potential future work on certain aspects of the study were also outlined.

In terms of future work, the results obtained using a non-classification method for optimisation of EMG electrode placement needs to be extended to different datasets. The robustness of the methods should be tested on EMG datasets of different data qualities, with different numbers of subjects. This ensures that research making use of this method will not generate poor quality EMG data, that could hamper further research efforts. To further extend the method, it can be applied to more subjects, and subjects with different EMG datasets. This ensures that the method is applicable to varying-application EMG datasets.

References

[1] Orthopaedic Trauma Institute, "Transradial Amputation - Orthopaedic Trauma Institute (OTI)," *Orthopaedic Trauma Institute (OTI)*. .

[2] C. Sollerman and A. Ejeskär, "Sollerman hand function test: a standardised method and its use in tetraplegic patients," *Scand. J. Plast. Reconstr. Surg. Hand Surg.*, vol. 29, no. 2, pp. 167–176, 1995.

[3] G. C. Matrone, C. Cipriani, E. L. Secco, G. Magenes, and M. C. Carrozza, "Principal components analysis based control of a multi-dof underactuated prosthetic hand," *J. NeuroEngineering Rehabil.*, vol. 7, p. 16, Apr. 2010.

[4] G. Magenes, F. Passaglia, and E. L. Secco, "A new approach of multi-d.o.f. prosthetic control," in *2008 30th Annual International Conference of the IEEE Engineering in Medicine and Biology Society*, 2008, pp. 3443–3446.

[5] A. Adewuyi, L. Hargrove, and T. Kuiken, "An Analysis of Intrinsic and Extrinsic Hand Muscle EMG for Improved Pattern Recognition Control," *IEEE Trans. Neural Syst. Rehabil. Eng.*, vol. PP, no. 99, pp. 1–1, 2015.

[6] M. Santello, M. Flanders, and J. F. Soechting, "Postural Hand Synergies for Tool Use," *J. Neurosci.*, vol. 18, no. 23, pp. 10105–10115, Dec. 1998.

[7] J. R. Napier, "The Prehensile Movements of the Human Hand," *Bone Jt. J.*, vol. 38–B, no. 4, pp. 902–913, Nov. 1956.

[8] K. Englehart, B. Hudgins, P. A. Parker, and M. Stevenson, "Classification of the myoelectric signal using time-frequency based representations," *Med. Eng. Phys.*, vol. 21, no. 6–7, pp. 431–438, Jul. 1999.

[9] Y. Fang and H. Liu, "Robust sEMG electrodes configuration for pattern recognition based prosthesis control," in *2014 IEEE International Conference on Systems, Man and Cybernetics (SMC)*, 2014, pp. 2210–2215.

[10] D. R. Merrill, J. Lockhart, P. R. Troyk, R. F. Weir, and D. L. Hankin, "Development of an Implantable Myoelectric Sensor for Advanced Prosthesis Control," *Artif. Organs*, vol. 35, no. 3, pp. 249–252, Mar. 2011.

[11] T. R. Farrell and R. F. Weir, "Pilot comparison of surface vs. implanted EMG for multifunctional prosthesis control," in *9th International Conference on Rehabilitation Robotics, 2005. ICORR 2005*, 2005, pp. 277–280.

[12] E. Criswell, *CRAM's INTRODUCTION TO Surface Electromyography*. Jones and Bartlett Publishers.

[13] G. C. Matrone, C. Cipriani, M. C. Carrozza, and G. Magenes, "Real-time myoelectric control of a multi-fingered hand prosthesis using principal components analysis," *J. NeuroEngineering Rehabil.*, vol. 9, p. 40, Jun. 2012.

[14] P. Shenoy, K. J. Miller, B. Crawford, and R. P. N. Rao, "Online Electromyographic Control of a Robotic Prosthesis," *IEEE Trans. Biomed. Eng.*, vol. 55, no. 3, pp. 1128–1135, Mar. 2008.

[15] R. Kato, T. Fujita, H. Yokoi, and T. Arai, "Adaptable EMG Prosthetic Hand using On-line Learning Method -Investigation of Mutual Adaptation between Human and Adaptable Machine," in *The 15th IEEE International Symposium on Robot and Human Interactive Communication, 2006. ROMAN 2006*, 2006, pp. 599–604.

[16] F. Tenore, A. Ramos, A. Fahmy, S. Acharya, R. Etienne-Cummings, and N. V. Thakor, "Towards the Control of Individual Fingers of a Prosthetic Hand Using Surface EMG Signals," in *29th Annual International Conference of the IEEE Engineering in Medicine and Biology Society, 2007. EMBS 2007*, 2007, pp. 6145–6148.

[17] A. Andrews, E. Morin, and L. McLean, "Optimal Electrode Configurations for Finger Movement Classification using EMG," in *2009 Annual International Conference of the IEEE Engineering in Medicine and Biology Society*, 2009, pp. 2987–2990.

[18] A. d'Avella, "Decomposition of EMG patterns as combinations of time-varying muscle synergies," in *First International IEEE EMBS Conference on Neural Engineering, 2003. Conference Proceedings*, 2003, pp. 55–58.

[19] L. J. Hargrove, K. Englehart, and B. Hudgins, "A Comparison of Surface and Intramuscular Myoelectric Signal Classification," *IEEE Trans. Biomed. Eng.*, vol. 54, no. 5, pp. 847–853, May 2007.

[20] C. Cipriani *et al.*, "Online Myoelectric Control of a Dexterous Hand Prosthesis by Transradial Amputees," *IEEE Trans. Neural Syst. Rehabil. Eng.*, vol. 19, no. 3, pp. 260–270, Jun. 2011.

[21] A. J. Young, L. H. Smith, E. J. Rouse, and L. J. Hargrove, “Classification of Simultaneous Movements Using Surface EMG Pattern Recognition,” *IEEE Trans. Biomed. Eng.*, vol. 60, no. 5, pp. 1250–1258, May 2013.

[22] M. Oskoei and H. Hu, “Myoelectric control systems—A survey.”

[23] G. Bosco, “Principal component analysis of electromyographic signals: an overview,” *Open Rehabil. J.*, vol. 3, no. 1, 2010.

[24] J. Segil, R. F. Weir, and D. Reamon, “Design of a myoelectric controller for a multi-DOF prosthetic hand based on principal component analysis,” 2011.

[25] K. A. Farry, I. D. Walker, and R. G. Baraniuk, “Myoelectric teleoperation of a complex robotic hand,” *IEEE Trans. Robot. Autom.*, vol. 12, no. 5, pp. 775–788, Oct. 1996.

[26] R. N. Khushaba and S. Kodagoda, “Electromyogram (EMG) feature reduction using mutual components analysis for multifunction prosthetic fingers control,” in *Control Automation Robotics & Vision (ICARCV), 2012 12th International Conference on*, 2012, pp. 1534–1539.

[27] A. d’Avella, P. Saltiel, and E. Bizzi, “Combinations of muscle synergies in the construction of a natural motor behavior,” *Nat. Neurosci.*, vol. 6, no. 3, pp. 300–308, Mar. 2003.

[28] G. Tsenov, A. H. Zeghbib, F. Palis, N. Shoylev, and V. Mladenov, “Neural Networks for Online Classification of Hand and Finger Movements Using Surface EMG signals,” in *2006 8th Seminar on Neural Network Applications in Electrical Engineering*, 2006, pp. 167–171.

[29] D. Peleg, E. Braiman, E. Yom-Tov, and G. F. Inbar, “Classification of finger activation for use in a robotic prosthesis arm,” *IEEE Trans. Neural Syst. Rehabil. Eng.*, vol. 10, no. 4, pp. 290–293, Dec. 2002.

[30] S. N. Sidek and A. J. H. Mohideen, “Mapping of EMG signal to hand grip force at varying wrist angles,” in *2012 IEEE EMBS Conference on Biomedical Engineering and Sciences (IECBES)*, 2012, pp. 648–653.

[31] J. F. Soechting and M. Flanders, “Flexibility and repeatability of finger movements during typing: analysis of multiple degrees of freedom,” *J. Comput. Neurosci.*, vol. 4, no. 1, pp. 29–46, Jan. 1997.

[32] R. Khushaba, “Electromyogram (EMG) Repository,” *Dr. Rami Khushaba*. [Online]. Available: http://www.rami-khushaba.com/electromyogram-emg-repository.html. [Accessed: 14-Jul-2016].

[33] N. Celadon, S. Dosen, M. Paleari, D. Farina, and P. Ariano, “Individual finger classification from surface EMG: Influence of electrode set,” in *2015 37th Annual International Conference of the IEEE Engineering in Medicine and Biology Society (EMBC)*, 2015, pp. 7284–7287.

[34] N. Uchida, A. Hiraiwa, N. Sonehara, and K. Shimohara, “EMG pattern recognition by neural networks for multi fingers control,” in *1992 14th Annual International Conference of the IEEE Engineering in Medicine and Biology Society*, 1992, vol. 3, pp. 1016–1018.

[35] A. Khorshidtalab, M. J. E. Salami, and M. Hamedi, “Evaluating the effectiveness of time-domain features for motor imagery movements using SVM,” in *2012 International Conference on Computer and Communication Engineering (ICCCE)*, 2012, pp. 909–913.

[36] A. Phinyomark, P. Phukpattaranont, and C. Limsakul, “Feature reduction and selection for EMG signal classification,” *Expert Syst. Appl.*, vol. 39, no. 8, pp. 7420–7431, Jun. 2012.

[37] Y. H. Liu and H. P. Huang, “Towards a high-stability EMG recognition system for prosthesis control: A one-class classification based non-target EMG pattern filtering scheme,” in *IEEE International Conference on Systems, Man and Cybernetics, 2009. SMC 2009*, 2009, pp. 4752–4757.

[38] M. A. Oskoei and H. Hu, “Support Vector Machine-Based Classification Scheme for Myoelectric Control Applied to Upper Limb,” *IEEE Trans. Biomed. Eng.*, vol. 55, no. 8, pp. 1956–1965, Aug. 2008.

[39] T. Kondo, O. Amagi, and T. Nozawa, “Proposal of anticipatory pattern recognition for EMG prosthetic hand control,” in *IEEE International Conference on Systems, Man and Cybernetics, 2008. SMC 2008*, 2008, pp. 897–902.

[40] P. M. Baggenstoss, “Class-specific classifier: avoiding the curse of dimensionality,” *IEEE Aerosp. Electron. Syst. Mag.*, vol. 19, no. 1, pp. 37–52, Jan. 2004.

[41] A. Andrews, “Finger Movement Classification Using Forearm EMG Signals.”

[42] H. Abdi and L. J. Williams, “Principal component analysis,” *Wiley Interdiscip. Rev. Comput. Stat.*, vol. 2, no. 4, pp. 433–459, Jul. 2010.

[43] L. J. Hargrove, Guanglin Li, K. B. Englehart, and B. S. Hudgins, “Principal Components Analysis Preprocessing for Improved Classification Accuracies in Pattern-Recognition-Based Myoelectric Control,” *IEEE Trans. Biomed. Eng.*, vol. 56, no. 5, pp. 1407–1414, May 2009.

[44] L. I. Smith, “A tutorial on Principal Components Analysis,” 2002.

[45] S. Dray, “On the number of principal components: A test of dimensionality based on measurements of similarity between matrices,” *Comput. Stat. Data Anal.*, vol. 52, no. 4, pp. 2228–2237, Jan. 2008.

[46] K. Moore, A. Dalley, and A. Agur, *Moore Clinically Orientated Anatomy*, 7th ed. Lippincott Williams and Wilkins.

[47] W. A. Lee, “Neuromotor synergies as a basis for coordinated intentional action,” *J. Mot. Behav.*, vol. 16, no. 2, pp. 135–170, Jun. 1984.

[48] P. K. Artemiadis and K. J. Kyriakopoulos, “EMG-Based Control of a Robot Arm Using Low-Dimensional Embeddings,” *IEEE Trans. Robot.*, vol. 26, no. 2, pp. 393–398, Apr. 2010.

[49] Q. Zhang, C. Zheng, and C. Xiong, “EMG-based estimation of shoulder and elbow joint angles for intuitive myoelectric control,” in *2015 IEEE International Conference on Cyber Technology in Automation, Control, and Intelligent Systems (CYBER)*, 2015, pp. 1912–1916.

[50] M. Borenstein, L. V. Hedges, J. P. T. Higgins, and H. R. Rothstein, “A basic introduction to fixed-effect and random-effects models for meta-analysis,” *Res. Synth. Methods*, vol. 1, no. 2, pp. 97–111, Apr. 2010.

[51] J. C. Lingoes and P. H. Schönemann, “Alternative measures of fit for the Schönemann-carroll matrix fitting algorithm,” *Psychometrika*, vol. 39, no. 4, pp. 423–427, Dec. 1974.

[52] Penn State, “Lesson 1.5: Additional Measures of Dispersion | STAT 505.” [Online]. Available: https://onlinecourses.science.psu.edu/stat505/node/21. [Accessed: 30-May-2017].

[53] U. Lorenzo-Seva, “How to report the percentage of explained common variance in exploratory factor analysis,” *Available Ftp Httppsico Fcep Urv*, 2013.

[54] M. Spüler, A. Sarasola-Sanz, N. Birbaumer, W. Rosenstiel, and A. Ramos-Murguialday, “Comparing metrics to evaluate performance of regression methods for decoding of neural signals,” in *2015 37th Annual International Conference of the IEEE Engineering in Medicine and Biology Society (EMBC)*, 2015, pp. 1083–1086.

[55] K. Padmavathi and K. S. R. Krishna, “Myocardial infarction detection using magnitude squared coherence and Support Vector Machine,” in *2014 International Conference on Medical Imaging, m-Health and Emerging Communication Systems (MedCom)*, 2014, pp. 382–385.

[56] N. R. Watson, C. K. Ying, and C. P. Arnold, “A global power quality index for aperiodic waveforms,” in *Ninth International Conference on Harmonics and Quality of Power. Proceedings (Cat. No.00EX441)*, 2000, vol. 3, pp. 1029–1034 vol.3.

[57] M. A. Motin, C. K. Karmakar, and M. Palaniswami, “An EEMD-PCA approach to extract heart rate, respiratory rate and respiratory activity from PPG signal,” in *2016 38th Annual International Conference of the IEEE Engineering in Medicine and Biology Society (EMBC)*, 2016, pp. 3817–3820.

[58] H. Carter, *Flexor digitorum superficialis muscle (plate 414), Anatomy of the Human Body (Henry Gray, 1918) Sourced from Wikimedia Commons*. 2017.

[59] H. Carter, *Flexor digitorum profundis muscle, (plate 415), Anatomy of the Human Body (Henry Gray, 1918) Sourced from Wikimedia Commons*. 2017.

[60] H. Carter, *Extensor carpi radialis longus muscle, (plate 418), Anatomy of the Human Body (Henry Gray, 1918) Sourced from Wikimedia Commons*. 2017.

[61] G. R. Naik, K. G. Baker, and H. T. Nguyen, “Dependence Independence Measure for Posterior and Anterior EMG Sensors Used in Simple and Complex Finger Flexion Movements: Evaluation Using SDICA,” *IEEE J. Biomed. Health Inform.*, vol. 19, no. 5, pp. 1689–1696, Sep. 2015.

[62] G. D. Eisenberg, K. G. H. M. Fyvie, and A.-K. Mohamed, “Real-Time Segmentation and Feature Extraction of Electromyography: Towards Control of a Prosthetic Hand,” *IFAC-Pap.*, vol. 50, no. 2, pp. 151–156, Dec. 2017.

Appendix A – Ethics Clearance Certification

R14/49 Mr Kyle Fyvie

HUMAN RESEARCH ETHICS COMMITTEE (MEDICAL)

CLEARANCE CERTIFICATE NO. M161180

NAME: (Principal Investigator)	Mr Kyle Fyvie
DEPARTMENT:	School of Electrical and Information Engineering
PROJECT TITLE:	Optimisation of Pre-Set Forearm Electromyographic Electrode Combinations using Principal Component Analysis
DATE CONSIDERED:	25/11/2016
DECISION:	Approved unconditionally
CONDITIONS:	
SUPERVISOR:	Mr Abdul-Khaaliq Mohamed
APPROVED BY:	Professor P Cleaton-Jones, Chairperson, HREC (Medical)
DATE OF APPROVAL:	30/11/2016

UNIVERSITY OF THE WITWATERSRAND, JOHANNESBURG
OFFICE OF THE DEPUTY VICE CHANCELLOR RESEARCH
18 JAN 2017
RESEARCH OFFICE RECEIVED

This clearance certificate is valid for 5 years from date of approval. Extension may be applied for.

DECLARATION OF INVESTIGATORS

To be completed in duplicate and **ONE COPY** returned to the Research Office Secretary in Room 301, Third Floor, Faculty of Health Sciences, Phillip Tobias Building, 29 Princess of Wales Terrace, Parktown, 2193, University of the Witwatersrand. I/we fully understand the conditions under which I am/we are authorized to carry out the above-mentioned research and I/we undertake to ensure compliance with these conditions. Should any departure be contemplated, from the research protocol as approved, I/we undertake to resubmit the application to the Committee. **I agree to submit a yearly progress report**. The date for annual re-certification will be one year after the date of convened meeting where the study was initially reviewed. In this case, the study was initially reviewed in November and will therefore be due in the month of November each year. Unreported changes to the application may invalidate the clearance given by the HREC (Medical).

Principal Investigator Signature

Date 18/01/2017

PLEASE QUOTE THE PROTOCOL NUMBER IN ALL ENQUIRIES